

RESEARCH ARTICLE

Semaphorin 6B acts as a receptor in post-crossing commissural axon guidance

Irwin Andermatt¹, Nicole H. Wilson¹, Timothy Bergmann¹, Olivier Mauti¹, Matthias Gesemann¹, Shanthini Sockanathan² and Esther T. Stoeckli^{1,*}

ABSTRACT

Semaphorins are a large family of axon guidance molecules that are known primarily as ligands for plexins and neuropilins. Although class-6 semaphorins are transmembrane proteins, they have been implicated as ligands in different aspects of neural development, including neural crest cell migration, axon guidance and cerebellar development. However, the specific spatial and temporal expression of semaphorin 6B (Sema6B) in chick commissural neurons suggested a receptor role in axon guidance at the spinal cord midline. Indeed, in the absence of Sema6B, post-crossing commissural axons lacked an instructive signal directing them rostrally along the contralateral floorplate border, resulting in stalling at the exit site or even caudal turns. Truncated Sema6B lacking the intracellular domain was unable to rescue the loss-of-function phenotype, confirming a receptor function of Sema6B. In support of this, we demonstrate that Sema6B binds to floorplate-derived plexin A2 (PlxnA2) for navigation at the midline, whereas a cis-interaction between PlxnA2 and Sema6B on pre-crossing commissural axons may regulate the responsiveness of axons to floorplate-derived cues.

KEY WORDS: Spinal cord development, *In ovo* RNAi, Cis-interaction, PlexinA2, Chick

INTRODUCTION

During development, a large number of neurons must connect with their target cells to establish functional neural circuits. A well-orchestrated set of axon guidance cues and their receptors on growth cones directs axonal navigation through the pre-existing tissue. On their journey, axons contact one or several intermediate targets before they reach their final destination. The floorplate at the CNS midline is one such intermediate target, where commissural axons cross to the contralateral side and grow along the rostrocaudal axis (Nawabi and Castellani, 2011; Chédotal, 2011). Owing to their stereotypic trajectory, dII commissural axons are a well-studied model for axon guidance. A number of long-range guidance cues directing these axons ventrally toward the floorplate have been identified (Kennedy et al., 1994; Augsburger et al., 1999; Charron et al., 2003; Islam et al., 2009). Midline crossing is regulated by a shift from attraction to repulsion (Stoekli and Landmesser, 1995; Stoekli et al., 1997; Long et al., 2004; Sabatier et al., 2004; Mambetisaeva et al., 2005; Chen et al., 2008). Axonal repulsion is induced by the upregulation of Robo1 on the growth cone surface,

which allows for the detection of Slit, a negative floorplate-derived signal (Philipp et al., 2012). Axonal navigation at the floorplate exit site is subsequently directed by F-spondin (Burstyn-Cohen et al., 1999), SynCAMs/Nectin-like molecules (Niederkofler et al., 2010), MDGA2 (Joset et al., 2011), and the morphogens Wnts (Lyuksyutova et al., 2003; Domanitskaya et al., 2010) and sonic hedgehog (Shh) (Bourikas et al., 2005; Wilson and Stoekli, 2013).

Semaphorin-plexin signaling also has been implicated in guiding commissural axons (Zou et al., 2000; Nawabi et al., 2010). GDNF- and NrCAM-mediated inhibition of the protease calpain 1 stabilizes plexin A1 (PlxnA1) on the growth cone (Nawabi et al., 2010; Charoy et al., 2012). The receptor complex neuropilin 2-PlxnA1 triggers sensitivity to the repulsive function of Sema3B, thus expelling axons from the midline area. Interestingly, Shh is also involved in this switch by downregulating protein kinase A (PKA) activity and thus inducing growth cone sensitivity to midline-derived class-3 semaphorins (Parra and Zou, 2010).

In contrast to the well-studied class-3 semaphorins, much less is known about class-6 semaphorins (Pasterkamp and Kolodkin, 2003; Kolodkin and Tessier-Lavigne, 2011; Pasterkamp, 2012). Class-6 semaphorins are a family of four type-I transmembrane proteins that bind directly to class-A plexins (plexinAs) in a neuropilin-independent manner. They have mainly been implicated as ligands for plexinAs. For example, Sema6A and Sema6B are required in the navigation of cardiac neural crest cells. They interact with PlxnA2 for proper cardiac outflow tract formation (Toyofuku et al., 2008). In axon guidance, Sema6A and Sema6B cooperate in the regulation of hippocampal mossy fiber targeting via interactions with PlxnA2 and PlxnA4 (Suto et al., 2007; Tawarayama et al., 2010). Sema6A directs the growth of sensory and sympathetic neurons (Xu et al., 2000; Haklai-Topper et al., 2010), and Sema6A/PlxnA4 signaling regulates the dendritic development of motoneurons (Zhuang et al., 2009). Sema6A also regulates cerebellar granule cell migration by controlling nucleus-centrosome coupling (Kerjan et al., 2005; Renaud et al., 2008). At the optic chiasm, Sema6D interacts with PlxnA1 and NrCAM to promote midline crossing of retinal axons (Kuwajima et al., 2012).

Although class-6 semaphorins act as ligands in all these processes, their intracellular domains, which include Src homology-3 (SH3) and zyxin-like domains, also suggest receptor functions (Eckhardt et al., 1997; Klostermann et al., 2000; Toyofuku et al., 2004a; Kolodkin and Tessier-Lavigne, 2011; Pasterkamp, 2012). This idea is supported by the analysis of corticospinal tract formation in *Sema6a* knockout mice, in which Sema6A may guide axons in a cell-autonomous manner. However, Sema6A is also expressed in the surrounding area, making it impossible to distinguish between cell-autonomous versus non-autonomous functions (Leighton et al., 2001; Rünker et al., 2008). A receptor function for Sema6A was also suggested by our previous

¹Institute of Molecular Life Sciences and Neuroscience Center Zurich, Winterthurerstrasse 190, Zurich 8057, Switzerland. ²The Solomon H. Snyder Department of Neuroscience, Johns Hopkins University School of Medicine, 725 N. Wolfe Street, Baltimore, MD 21205, USA.

*Author for correspondence (esther.stoekli@imls.uzh.ch)

studies on boundary cap cell clustering (Mauti et al., 2007). Boundary cap cell clusters act as gate keepers, allowing axons, but not cell bodies, to cross the CNS/PNS boundary. After knocking down *Sema6A* in boundary cap cells, motoneurons migrated out of the spinal cord along the ventral roots. This phenotype could be explained by a model in which *Sema6A* is a receptor on migrating boundary cap cells that recognizes *PlxnA1* on motor axons as a stop signal. The *Sema6A-PlxnA1* interaction would lead to the accumulation of boundary cap cells and indirectly initiate their clustering at the ventral motor exit point (Mauti et al., 2007).

So far, the only direct evidence for a receptor function of class-6 semaphorins *in vivo* comes from heart development, where *Sema6D* was shown to be a ligand and receptor for *PlxnA1* (Toyofuku et al., 2004a,b).

Here, we demonstrate in chick that *Sema6B* is an axon guidance receptor. We show that *Sema6B* guides post-crossing commissural axons by binding to *PlxnA2* expressed by floorplate cells. In the absence of axonal *Sema6B* or its ligand *PlxnA2* in the floorplate, post-crossing commissural axons fail to turn rostrally along the longitudinal axis of the spinal cord.

RESULTS

Sema6b is transiently expressed in dorsal commissural neurons

Sema6b mRNA was readily detectable in dII commissural neurons of the chicken neural tube during the time window when their axons cross and exit the floorplate (Fig. 1A-F). Importantly, *Sema6b* mRNA was only detectable at HH22 (Fig. 1C), when most axons have reached the ipsilateral floorplate border. No *Sema6b* expression was detectable in commissural neurons at HH21, that is, shortly before their axons reach the floorplate (Fig. 1B,E). Highest expression levels were found at HH24, when commissural axons exit the floorplate and turn rostrally along the contralateral floorplate border (Fig. 1D,E). At later stages (not shown), *Sema6b* was found at lower levels throughout the gray matter, consistent with findings in mouse (Suto et al., 2005). The identity of dII neurons was confirmed by labeling adjacent sections with probes for the marker *Lhx2/9* (Helms and Johnson, 2003) (Fig. 1F,G).

As we described previously, *Sema6a* was not expressed in commissural neurons at the lumbar level (Mauti et al., 2007; but see

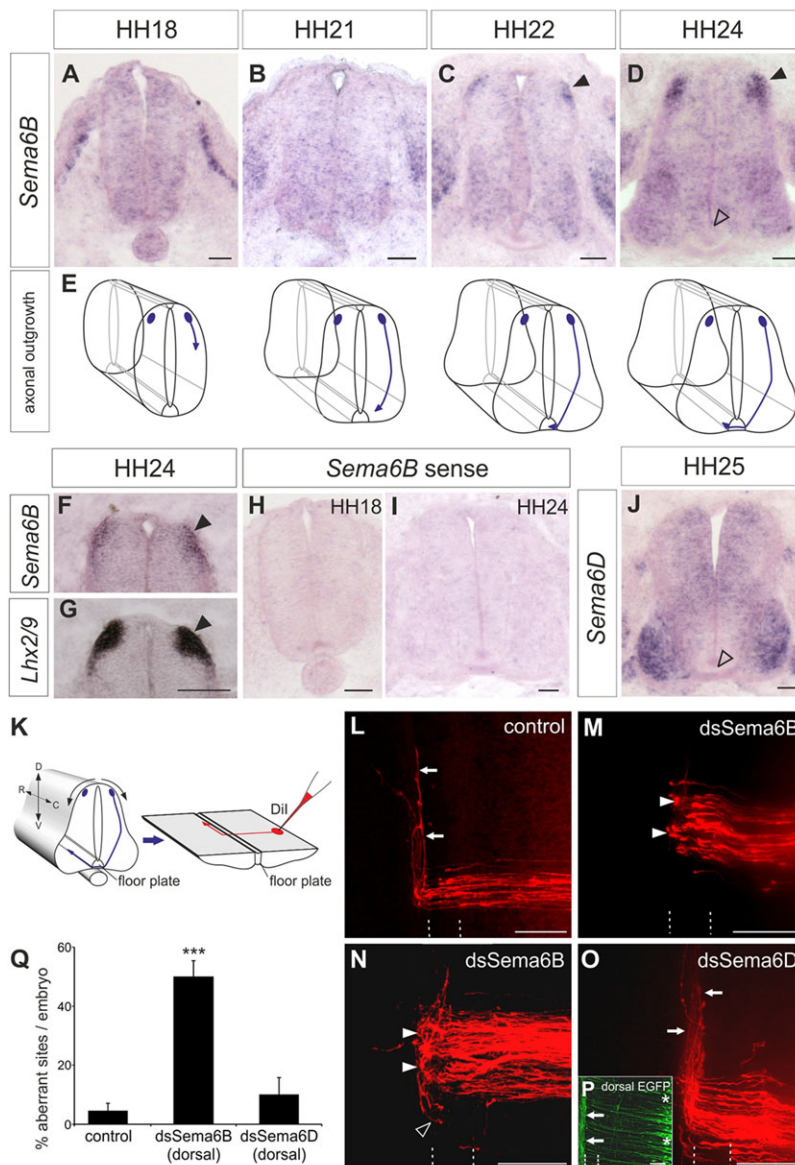


Fig. 1. *Sema6b* expression in dII commissural neurons peaks at HH24 and is required for post-crossing commissural axon guidance. (A-E) Expression of *Sema6b* mRNA in transverse sections of the chicken lumbar spinal cord at the indicated developmental stages (A-D) with schematic representations of the corresponding growth of dII axons (E). *Sema6b* is first detected in dII neurons at HH22, when their axons have reached the ipsilateral floorplate border (C, arrowhead). Expression of *Sema6b* in dII neurons is strongest at HH24 (D, arrowheads). (F,G) Probing adjacent sections with *Lhx2/9* confirmed that *Sema6b* is expressed in dII neurons (arrowheads). (H,I) No staining is seen with a *Sema6b* sense probe. (J) Diffuse expression of *Sema6d* at HH25, with higher levels in motoneurons. Neither *Sema6b* nor *Sema6d* is expressed in the floorplate (D,J, open arrowheads). (K) Schematic of an open-book preparation and application of Dil for axonal tracing (red). D, dorsal; V, ventral; R, rostral; C, caudal. (L) Commissural axons cross the midline and extend along the contralateral floorplate border (arrows) in untreated control embryos. (M,N) After silencing *Sema6B* by injection and electroporation of dsRNA (*dsSema6b*), axons stall at the contralateral floorplate border (closed arrowheads) or even turn caudally (open arrowhead). (O) Silencing *Sema6D* by injection and electroporation of dsRNA (*dsSema6d*) did not affect axon guidance (arrows). (P) Expression of a co-electroporated EGFP reporter confirmed the exclusively dorsal targeting of dsRNA (asterisks). Arrows mark axons of contralaterally projecting commissural neurons. The floorplate is indicated by dashed lines. (Q) Quantification of Dil injection sites with aberrant axonal pathfinding. *** $P < 0.001$; error bars indicate s.e.m. Scale bars: 50 μm in A-D,F-J; 100 μm in L-P.

dorsal expression at the brachial level described by Toyofuku et al., 2008). *Sema6d* was strongly expressed in motor neurons and at lower levels in the spinal cord gray matter (Fig. 1J) (Mauti et al., 2007). No class-6 semaphorins were expressed in the floorplate (Fig. 1) (Mauti et al., 2007). No ortholog of *Sema6c* is found in the chicken genome.

Loss of *Sema6B* causes defects in commissural axon guidance

The transient expression of *Sema6b* in dII neurons during the window of axonal midline crossing and turning suggested a role for *Sema6B* in axonal pathfinding. To test this hypothesis, we used *in ovo* RNAi to knock down *Sema6B* in commissural neurons (Fig. 1K–Q). Long dsRNA derived from *Sema6b* or *Sema6d*, together with an EGFP reporter plasmid, was injected into the central canal at HH18 and electroporated into the dorsal spinal cord (Fig. 1P). Commissural axon pathfinding was assessed 2 days later by axonal tracing with lipophilic DiI applied to the cell bodies of dII neurons (Fig. 1K–O).

In untreated control embryos, commissural axons crossed the floorplate and turned rostrally along the contralateral floorplate border (Fig. 1L,Q; $95.3 \pm 2.5\%$ of DiI sites were normal; $n=19$ embryos, $N=164$ DiI injection sites). When *Sema6B* was downregulated, axons failed to turn rostrally and instead stalled or even turned caudally at the floorplate exit site in $50.1 \pm 5.4\%$ of the DiI sites ($n=22$, $N=149$; Fig. 1M,N,Q). By contrast, loss of *Sema6D* did not affect the guidance of post-crossing axons (abnormalities at only $10.2 \pm 5.7\%$ of injection sites; $n=13$, $N=84$; Fig. 1O,Q). Taken together, these experiments indicated that downregulation of *Sema6B* specifically interfered with commissural axon guidance upon floorplate exit.

Sema6B acts as a receptor in commissural axons

Semaphorins are typically known as ligands for plexin receptors. However, *Sema6b* was expressed in commissural neurons but not in the floorplate, suggesting a role for the protein as receptor rather than ligand. To test this idea, we asked whether a truncated version of *Sema6B* lacking the intracellular domain could rescue the axon guidance defects induced by *Sema6B* knockdown. Here, we used artificial microRNAs (miRNAs) to knock down *Sema6B*, and then expressed knockdown-resistant forms of *Sema6B* in commissural neurons (Fig. 2A). The efficiency of the *Sema6B* miRNA (miS6B) and rescue constructs (*Sema6B*ΔmiR) were verified *in vivo* and *in vitro* (supplementary material Fig. S1A–E).

In control embryos expressing a miRNA against Luciferase (miLuc) in the dorsal spinal cord, normal turning of post-crossing commissural axons was observed at $69.5 \pm 6.4\%$ of injection sites ($n=9$, $N=69$; Fig. 2B,H). However, only $20.8 \pm 6.6\%$ of injection sites showed normal axon pathfinding after downregulation of *Sema6B* with miS6B ($n=10$, $N=81$; Fig. 2C,H). In agreement with its temporal expression pattern, loss of *Sema6B* did not affect commissural axon guidance towards the ventral midline (supplementary material Fig. S3). These results were in line with our previous experiments in which *Sema6B* was downregulated with long dsRNA (Fig. 1). The turning defects of post-crossing axons observed after silencing of *Sema6B* could be rescued by the concomitant expression of *Sema6B*ΔmiR (Fig. 2D,H). Normal axonal pathfinding in the rescue condition was observed at $58.2 \pm 7.7\%$ of injection sites ($n=13$, $N=91$). By contrast, expression of *Sema6B*ΔCTΔmiR, a truncated version of *Sema6B* lacking the cytoplasmic domain, was unable to rescue commissural axon guidance, as only $21.5 \pm 6.2\%$ of injection sites ($n=15$, $N=84$)

were normal (Fig. 2E,H). Expression of *Sema6B* alone did not significantly change axon pathfinding (Fig. 2F,H; $47.3 \pm 7.4\%$ normal DiI sites; $n=13$, $N=101$). By contrast, expression of *Sema6B*ΔCTΔmiR resulted in aberrant post-crossing axon pathfinding (Fig. 2G,H; $25.6 \pm 6.8\%$ normal DiI sites; $n=9$, $N=61$), suggesting that *Sema6B*ΔCTΔmiR acts in a dominant-negative manner. Taken together, these results demonstrate that the intracellular portion of *Sema6B* is crucial for correct navigation of commissural axons and that *Sema6B* functions cell-autonomously as an axon guidance receptor.

PlxnA2 is a potential interaction partner for *Sema6B* in commissural axon guidance

We next sought a potential floorplate-derived ligand for the *Sema6B* receptor. Based on the known interactions of class-6 semaphorins with plexinAs (Suto et al., 2005; Mauti et al., 2007; Toyofuku et al., 2008), we assessed the expression patterns of plexinAs during commissural axon pathfinding. As we described previously (Mauti et al., 2006), plexins have dynamic and distinct expression patterns in the chicken lumbar spinal cord (Fig. 3). At HH21, just before the first dII commissural axons reach the floorplate at lumbar levels of the spinal cord, *Plxna1* was strongly expressed in the ventral spinal cord (including the floorplate), and at lower levels throughout the rest of the neural tube (Fig. 3A). By HH25, *Plxna1* expression was high in dII neurons and in motoneurons (Fig. 3A'), but was no longer expressed in the floorplate (inset in Fig. 3A'). *Plxna2* was expressed strongly in dII neurons and the floorplate at both HH21 and HH25 (Fig. 3B,B'). *Plxna4* was expressed in dII neurons, but was not found in the floorplate (Fig. 3C,C'). By contrast, *Plxnc1* was found in the floorplate (Fig. 3D,D'). No ortholog of *Plxna3* is found in the chicken genome.

Consistent with their potential role as interaction partners for *Sema6B*, unilateral downregulation of plexinAs interfered with commissural axon pathfinding (Fig. 3E–H). The loss of *PlxnA1* caused post-crossing defects at $43.8 \pm 7.3\%$ of DiI sites ($n=16$, $N=106$; Fig. 3E,M). After downregulation of *PlxnA2*, post-crossing commissural axons failed to turn rostrally at $54.1 \pm 9.1\%$ of injection sites ($n=15$, $N=92$; Fig. 3F,M). The same phenotype was observed at $46.3 \pm 11.3\%$ of injection sites after downregulation of *PlxnA4* ($n=11$, $N=66$; Fig. 3G,M).

Based on these results, we analyzed the requirement for plexinAs in post-crossing commissural axon guidance more specifically by targeted electroporation of the floorplate (Fig. 3I–L). Because *Plxna1* expression disappeared from the floorplate during axonal crossing and turning, and based on biochemical interaction assays that indicated that *PlxnA1* did not bind to *Sema6B* (Toyofuku et al., 2008; and see below), we instead considered *PlxnA2* as the most likely binding partner for axonal *Sema6B* in the floorplate. Indeed, after knocking down *PlxnA2* in the ventral spinal cord, we found contralateral stalling phenotypes comparable to those observed in the absence of *Sema6B* at $36.2 \pm 5.2\%$ of injection sites ($n=18$, $N=149$; Fig. 3I,N). By contrast, ventral electroporation of *Plxna4* dsRNA did not interfere with commissural axon guidance (Fig. 3J,N). As *Plxna4* was never found in the floorplate (Fig. 3C,C'), this experiment was a negative control. Aberrant axonal behavior was detected at only $5.0 \pm 2.6\%$ of injection sites ($n=7$, $N=56$). Downregulation of *PlxnC1*, which is expressed in the floorplate but interacts with class-7 semaphorins (Pasterkamp, 2012), did not interfere with commissural axon navigation: aberrant behavior was detected at only $5.8 \pm 4.1\%$ of injection sites ($n=12$, $N=75$; Fig. 3K,N). Together, the targeted electroporation experiments supported a specific axon guidance role of floorplate-derived *PlxnA2*.

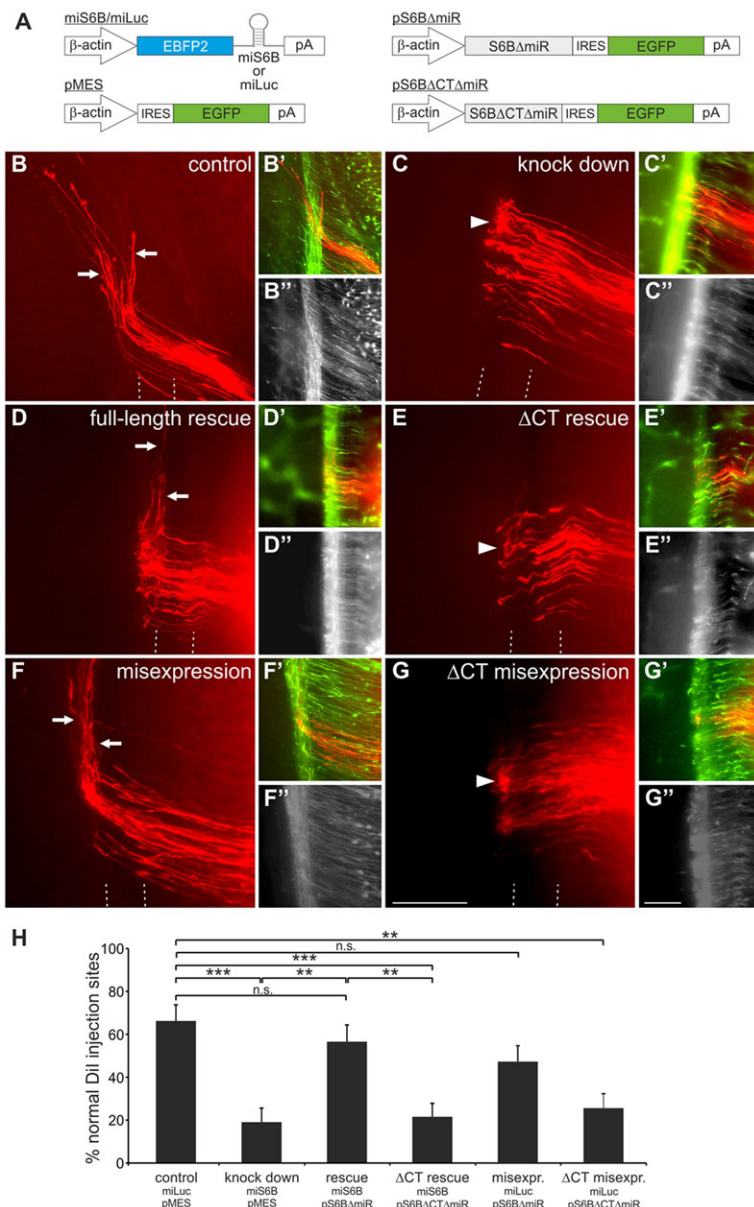


Fig. 2. The intracellular domain of Sema6B is essential for post-crossing commissural axon guidance. (A) Schematics of miRNA and rescue constructs used in B-H. (B-G') Open-book analysis of Dil injection sites in embryos co-electroporated with: (B) miLuc and pMES; (C) miS6B and pMES; (D) miS6B and pSema6BΔmiR; (E) miS6B and pSema6BΔCTΔmiR; (F) pSema6BΔmiR alone; or (G) pSema6BΔCTΔmiR alone. Arrows (B,D,F) indicate normal crossing and turning of commissural axons. Post-crossing axons that failed to turn correctly at the contralateral floorplate border are indicated by arrowheads (C,E,G). (B'-G') Merge of Dil-labeled axons (red) and EGFP (green) used to visualize the expression of pMES constructs. (B''-G'') Enhanced blue fluorescent protein-2 (EBFP2) visualizes the expression of miRNA constructs. The floorplate is indicated by dashed lines. Scale bars: 100 μm. (H) Quantification of Dil injection sites with normal axonal pathfinding. ***P*<0.01, ****P*<0.001; n.s., not significant; error bars indicate s.e.m.

The intracellular domain of PlxnA2 is dispensable for its axon guidance function in the floorplate

If PlxnA2 was acting as a floorplate-derived ligand for Sema6B during commissural axon guidance, then the cytoplasmic domain of PlxnA2 could be dispensable for its axon guidance activity in the floorplate. To test this idea, we downregulated PlxnA2 specifically in the floorplate using an miRNA (miPA2), then attempted to rescue the phenotype by expressing miRNA-resistant constructs encoding either the full-length protein (PlexinA2ΔmiR) or a truncated version containing the extracellular and the transmembrane domains but lacking the cytoplasmic tail (PlexinA2ΔCTΔmiR). The miRNA and rescue constructs were verified *in vivo* and *in vitro* (supplementary material Fig. S2). All constructs were under the control of a *Hoxa1* enhancer in order to drive specific expression in the floorplate (Fig. 4A) (Wilson and Stoeckli, 2011).

As expected, the miRNA-based knockdown of PlxnA2 specifically in the floorplate caused axon pathfinding errors. Whereas the control group injected and electroporated with miLuc and the EGFP plasmid showed normal axon guidance at 60.9±8.5%

of the injection sites per embryo ($n=12$ embryos, $N=107$ injection sites), downregulation of PlxnA2 specifically in the floorplate with miPA2 reduced normal axon guidance to only 30.6±6.1% of the injection sites ($n=14$, $N=97$). Axon guidance was rescued by co-injection and electroporation of knockdown-resistant full-length PlxnA2 (PlexinA2ΔmiR; normal axon guidance at 63.2±5.5% of the injection sites per embryo; $n=12$, $N=79$) and truncated PlxnA2 (PlexinA2ΔCTΔmiR; normal axon guidance at 54.2±5.1% of the injection sites per embryo; $n=17$, $N=119$). The integrity of the floorplate was not affected in these experiments, as the expression of neither markers (*Hnf3β* and *Nkx2.2*) nor other axon guidance molecules (*Shh* and *Slit2*) was perturbed (supplementary material Fig. S4).

Together, these results suggest that PlxnA2 acts directly as an axon guidance molecule in the floorplate. The extracellular domain of PlxnA2, and not its intracellular domain, is crucial for this function. This finding was consistent with our hypothesis that PlxnA2 is a floorplate-derived ligand for Sema6B during commissural axon guidance.

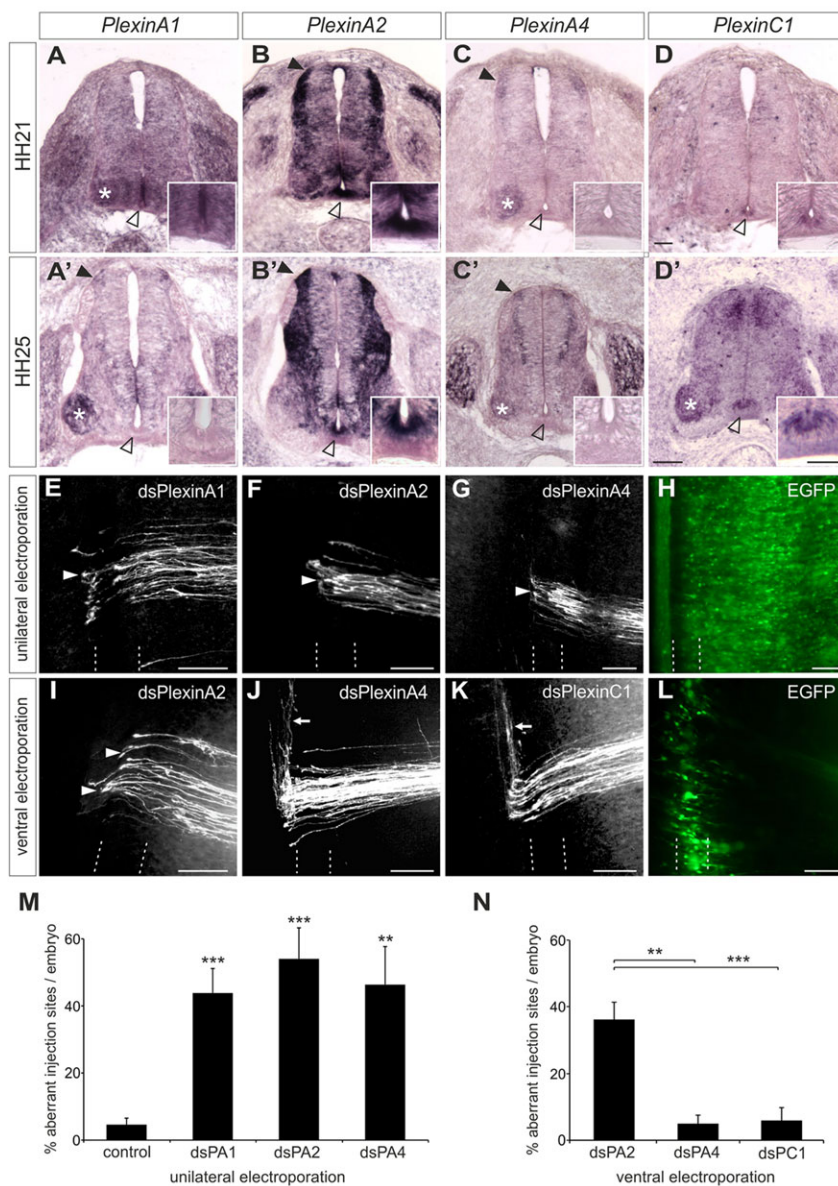


Fig. 3. For correct pathfinding, PlxnA2 is required in both commissural neurons and the floorplate.

(A-D') Expression patterns of plexins analyzed by *in situ* hybridization at stages HH21 (A-D) and HH25 (A'-D'). Staining in commissural neurons is indicated by closed arrowheads. Motoneurons are marked with asterisks. The floorplate is indicated by open arrowheads and shown at higher magnification in the insets. (E-G) After downregulation of PlxnA1 (E), PlxnA2 (F) or PlxnA4 (G) by unilateral electroporation of dsRNA, axons failed to turn rostrally at the contralateral floorplate border (arrowheads). (H) Only injection sites in the electroporated area (verified by EGFP expression) were included in the analysis. (I-K) Analysis of commissural axon pathfinding after downregulation of PlxnA2 (I), PlxnA4 (J) or PlxnC1 (K) exclusively in the ventral spinal cord. After ventral downregulation of PlxnA2 (I, arrowheads), post-crossing axons failed to turn into the longitudinal axis or even turned caudally. Axon guidance was unaffected after ventral downregulation of PlxnA4 (J, arrow) or PlxnC1 (K, arrow). (L) Successful and exclusive targeting of cells at the ventral midline was verified by EGFP expression. The floorplate is indicated by dashed lines. (M,N) Quantification of injection sites with aberrant axonal pathfinding after (M) unilateral or (N) ventral electroporation of dsRNA. *** $P < 0.001$; ** $P < 0.01$; error bars indicate s.e.m. Scale bars: 50 μm in A-D'; 100 μm in E-L.

Sema6B interacts with PlxnA2

To support the above hypothesis, we next confirmed a physical interaction between Sema6B and PlxnA2 in co-immunoprecipitation (co-IP) and binding assays. The co-IP of Sema6A with PlxnA2 was used as positive control, as this interaction has been described previously (Suto et al., 2005, 2007; Toyofuku et al., 2008; Janssen et al., 2010; Nogi et al., 2010). Immunoprecipitation of myc-tagged PlxnA2 ectodomains from conditioned medium was found to pull down both Sema6B-Fc and Sema6A-Fc ectodomains (Fig. 4F-I).

We confirmed the interaction between Sema6B and PlxnA2 by cell-binding assays. HEK293 cells expressing different class-6 semaphorins were incubated with PlxnA2 ectodomains fused to alkaline phosphatase (PlxnA2^{ecto}-AP; Fig. 4J-N). As expected, binding of PlxnA2^{ecto}-AP to Sema6A-expressing cells was very strong (Fig. 4J). PlxnA2^{ecto}-AP binding to Sema6B-expressing cells was clearly detectable, but weaker than to Sema6A-expressing cells (Fig. 4K). PlxnA2^{ecto}-AP also bound to Sema6B Δ CT (Fig. 4M). However, no binding of PlxnA2^{ecto}-AP was found to cells transfected with Sema6D (Fig. 4L) or a control EGFP plasmid

(Fig. 4N). By contrast, PlexinA1^{ecto}-AP bound to cells expressing Sema6A (Fig. 4O) and Sema6D (Fig. 4Q) but not to cells expressing Sema6B (Fig. 4P,R). Thus, we could exclude PlxnA1 as a Sema6B interaction partner. Taken together, our results confirmed a previously reported interaction between Sema6B and PlxnA2 (Toyofuku et al., 2008), and strongly supported our hypothesis that PlxnA2 is a floorplate-derived ligand for Sema6B during commissural axon guidance.

Sema6B mediates an outgrowth response of commissural neurons to PlxnA2

We next investigated whether the response of commissural axons to PlxnA2 substrate was altered by a lack of Sema6B (Fig. 5). On coverslips coated with Albumax, Laminin or concentrated conditioned medium from cells expressing either AP alone or PlexinA2^{ecto}-AP, we plated dissociated commissural neurons from embryos that were electroporated with a vector expressing EBFP2 and miS6B to knock down Sema6B. Because electroporation is not 100% efficient, the pools of commissural neurons obtained

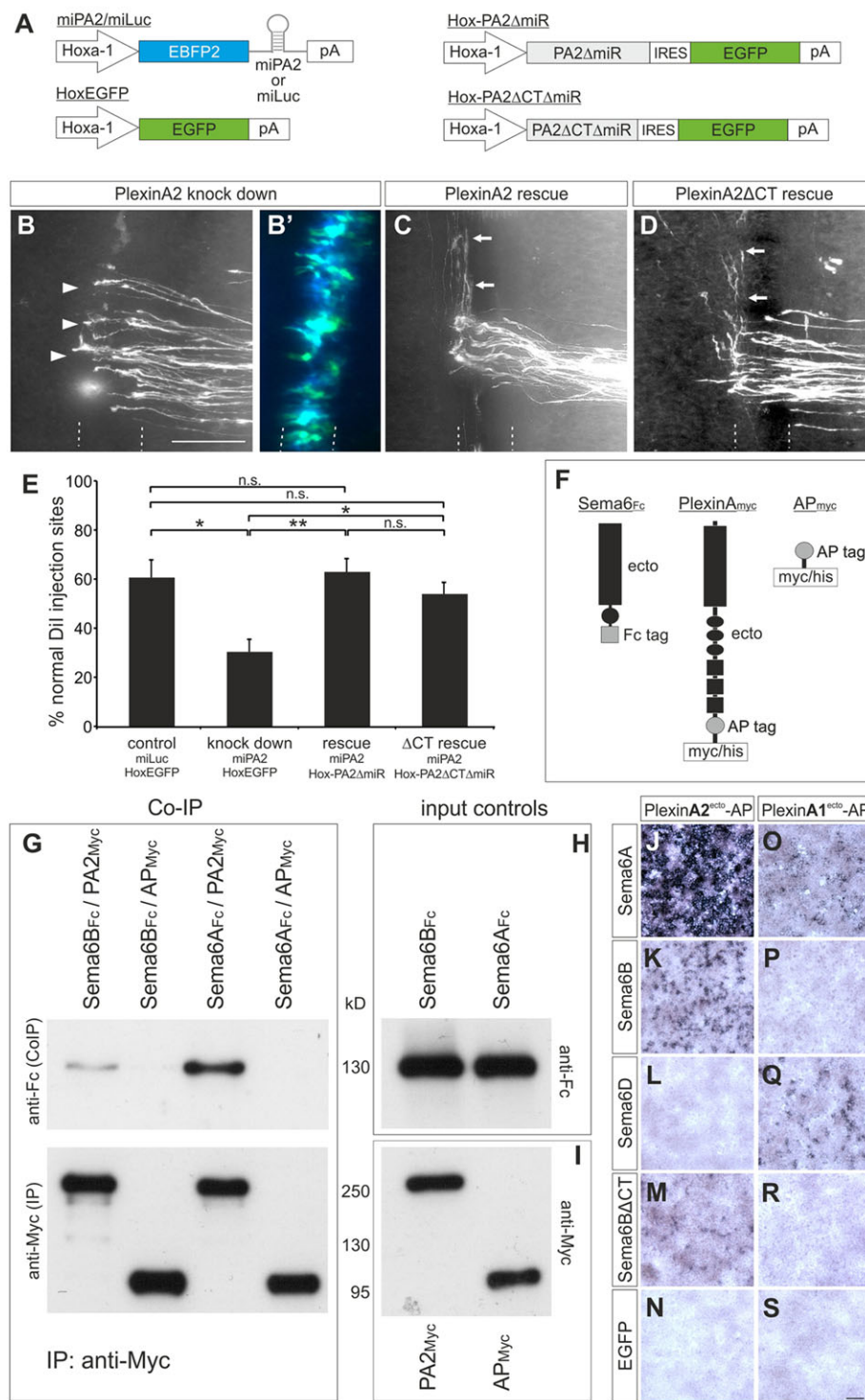


Fig. 4. The extracellular domain of PlxnA2 mediates its axon guidance activity in the floorplate and binds to Semaphorin 6B.

(A) Schematics of the constructs used in B-E. *Hoxa1* drives floorplate-specific expression. (B-D) Open-book analysis of embryos co-electroporated with: (B) miPA2 and Hox-EGFP; (C) miPA2 and Hox-PA2ΔmiR; or (D) miPA2 and Hox-PA2ΔCTΔmiR. (B') The successful and exclusive targeting of floorplate cells was confirmed by EGFP and EBFP2 fluorescence from the co-electroporated constructs. Post-crossing axons that failed to turn correctly at the contralateral floorplate border are indicated by arrowheads (B). Arrows (C,D) indicate normal crossing and turning of commissural axons. (E) Quantification of injection sites with normal axon pathfinding after floorplate-specific manipulations of PlxnA2. * $P < 0.05$, ** $P < 0.01$; n.s., not significant; error bars indicate s.e.m.

(F) Schematics of the proteins used for co-IPs. (G) Sema6B_{Fc} or Sema6A_{Fc} ectodomains were incubated with either PA2_{Myc} ectodomains or AP_{Myc} and immunoprecipitated with anti-myc agarose beads. Co-IP of Sema6B and Sema6A was detected with anti-Fc antibodies on western blots (upper panel). Blots stained with anti-myc antibodies, to demonstrate the successful immunoprecipitation, are shown below. As controls, the input proteins from conditioned media were analyzed on blots developed with (H) anti-Fc antibodies to detect Sema6B_{Fc} and Sema6A_{Fc} ectodomains and (I) anti-myc antibodies to detect PA2_{Myc} and AP_{Myc}. (J-S) HEK293T cells were transfected with chicken Sema6A (J,O), Sema6B (K,P), Sema6D (L,Q), Sema6BΔCT (M,R) or EGFP (N,S) and incubated with conditioned medium containing AP-tagged ectodomains of PlxnA2 (PlexinA2^{ecto}-AP, J-N) or PlxnA1 (PlexinA1^{ecto}-AP, O-S). Scale bars: 100 μm.

comprised both wild-type and miRNA-expressing (EBFP2-positive) neurons from the same embryos. Thus, the wild-type neurons provided an internal control. Cultures were allowed to grow for 48 h before fixation and immunolabeling for the axonal marker axonin 1 (contactin 2).

As expected, we observed modest outgrowth of commissural axons on Albumax (Fig. 5G; data not shown), whereas the Laminin and AP substrates encouraged slightly longer axons (Fig. 5A-D,G). By far the longest axons were found on PlxnA2-coated coverslips (Fig. 5E-G). However, the expression of miS6B (but not miLuc) significantly

dampened this outgrowth response to PlxnA2 (Fig. 5E-H). These results indicate that PlxnA2 promotes the outgrowth of commissural axons in a pathway that is mediated by Semaphorin 6B.

Axonal PlxnA2 contributes to post-crossing commissural axon guidance

Our functional analyses suggested that PlxnA2 is a floorplate-derived ligand for Semaphorin 6B during commissural axon guidance. However, *PlxnA2* was expressed not only in the floorplate but also in commissural neurons (Fig. 3B). Because PlxnA1 has previously

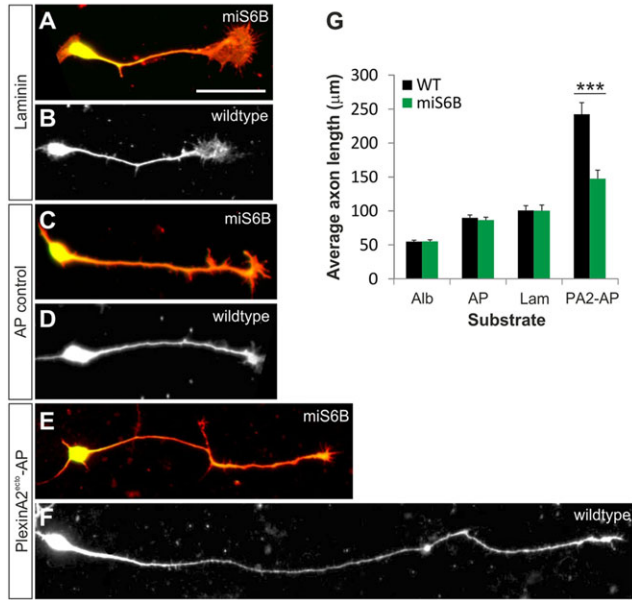


Fig. 5. The commissural axon response to PlxnA2 is Sema6B dependent. (A–F) Examples of axon outgrowth of commissural neurons obtained from embryos electroporated with βactin-EBFP2-miS6B on Laminin (A,B), AP only (C,D) and PlexinA2^{ecto}-AP (E,F). Axons were co-immunolabeled for axonin 1 and EBFP2. Co-labeled neurons appear yellow in A,C,E. Scale bar: 50 μm. (G) Quantification of axon lengths on different substrates after electroporation of βactin-EBFP2-miS6B. WT, wild type; Alb, Albumax; AP, concentrated conditioned medium from AP-expressing cells; Lam, Laminin; PA2-AP, concentrated conditioned medium from PlexinA2^{ecto}-AP-expressing cells. ****P*<0.001; error bars indicate s.e.m.

been identified as an axonally expressed receptor with important roles in commissural axon guidance (Nawabi et al., 2010; Charoy et al., 2012), we hypothesized that other plexinAs might function similarly. To test this idea, we knocked down PlxnA2 and PlxnA4 only in the dorsal spinal cord by targeted electroporation of long dsRNA. In line with results from unilateral electroporations, knockdown of PlxnA2 in commissural neurons perturbed axon guidance at 44.3±8.1% of injection sites (*n*=15 embryos, *N*=115 injection sites; Fig. 6A,D). Similarly, dorsal downregulation of PlxnA4 interfered with post-crossing axon guidance at 38.9±6.0% of injection sites (*n*=23, *N*=153; Fig. 6D). Based on these results, both PlxnA2 and PlxnA4 could act as guidance receptors on commissural axons after crossing the midline. Furthermore, these findings suggested the possibility of axonal cis-interactions with Sema6B.

To investigate this idea, we examined the localization patterns of Sema6B and plexinAs in more detail. *In vivo*, the expression of PlxnA2 was strongest on pre-crossing and commissural segments (Fig. 6E). Unfortunately, staining of Sema6B on sections was not possible with the available antibody, but our earlier *in situ* results (Fig. 1) suggested that *Sema6b* was only expressed in pre-crossing axons shortly before they contacted the floorplate. In cultured commissural neurons obtained from HH25 embryos, we found expression of Sema6B all along the axons and on growth cones (Fig. 6F). PlxnA2 (Fig. 6H,K) was expressed similarly. By contrast, PlxnA4 was found in a punctate pattern along the axons (Fig. 6I), suggesting an intracellular, vesicular localization. Additionally, only very low levels of PlxnA4 were found in growth cones (Fig. 6L), making the formation of a cis-complex with Sema6B on the growth cone or axonal surface unlikely.

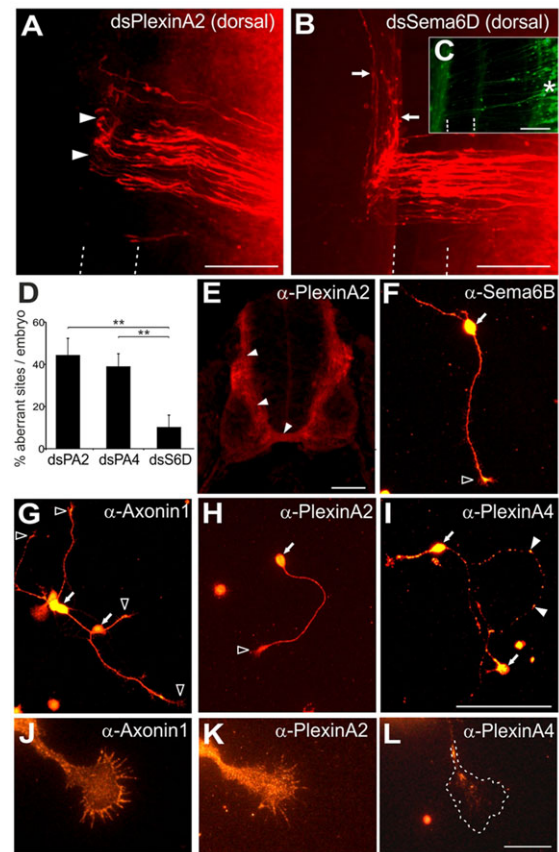


Fig. 6. Axonal PlxnA2 is required for the pathfinding of post-crossing axons. (A) Downregulation of PlxnA2 in the dorsal spinal cord led to aberrant commissural axon guidance at the contralateral floorplate border (arrowheads). (B) Commissural axon guidance was normal (arrows) when dsSema6D was electroporated dorsally. (C) Electroporation of only the dorsal spinal cord was verified by EGFP expression (asterisk). (D) Quantifications of Dil injection sites with aberrant axon pathfinding. ***P*<0.01; error bars indicate s.e.m. The dsSema6D value is taken from Fig. 1. (E) Staining of transverse sections of HH25 spinal cords localized PlxnA2 immunoreactivity to the pre-crossing segment and commissure (arrowheads). (F) Sema6B was expressed all along dissociated commissural axons and on growth cones (open arrowhead), as was axonin 1 (G,J), a marker for commissural neurons. PlxnA2 (H,K) was also expressed on axons and growth cones, in contrast to PlxnA4 (I) which was found in a punctate pattern along axons (arrowheads). No PlxnA4 was found on growth cones (L). Arrows (F–I) indicate neuronal soma. Scale bars: 100 μm in A–C,E; 50 μm in F–I; 20 μm in J–L.

Taken together, the co-expression of PlxnA2 and Sema6B in similar subcellular locations, together with their ability to interact with each other (Fig. 4; supplementary material Fig. S5), suggested a possible cis-interaction between these molecules on commissural axons as they enter and cross the floorplate.

PlxnA2 misexpression in commissural neurons leads to axon stalling in the dorsal neural tube

As knockdown of PlxnA2 in commissural neurons impaired axon guidance (Fig. 6), we tested whether it was required cell-autonomously for growth cone turning (Fig. 7; supplementary material Fig. S2). We used the previously described rescue constructs encoding either full-length PlxnA2 or PlexinA2ΔCT (supplementary material Fig. S2). This time, the miRNA and rescue constructs were driven by a dI1 neuron-specific enhancer of *Math1* (*Atoh1*) (Fig. 7A; supplementary material Fig. S2) (Helms and Johnson, 2003; Wilson and Stoeckli, 2011). However, the

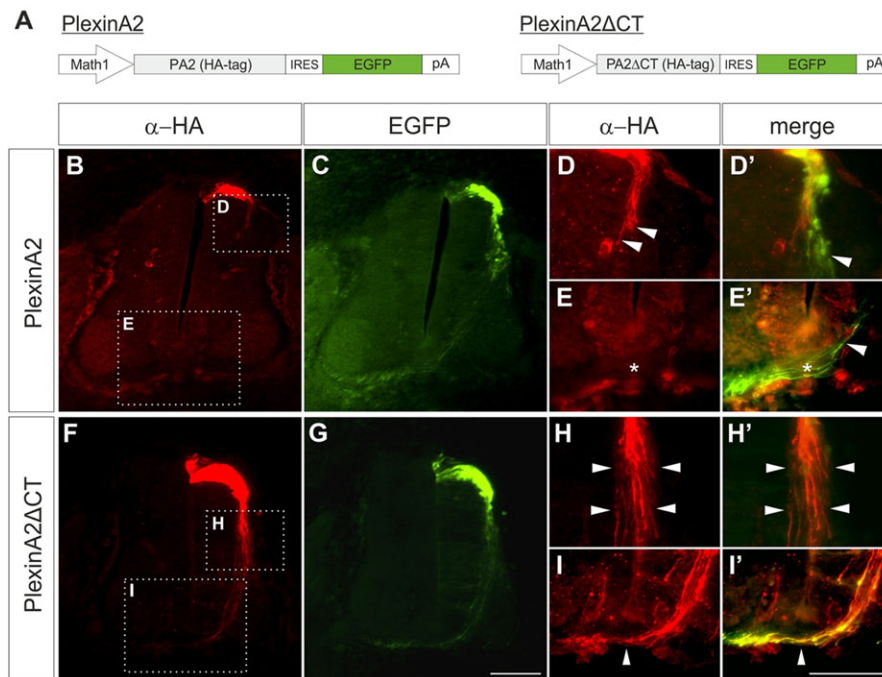


Fig. 7. Overexpression of full-length PlxnA2 prevents ventral growth of dl1 axons.

(A) Schematics of the constructs used in B-I. *Math1* drives dl1 neuron-specific expression. Axon growth was assessed by (B,F) anti-HA immunolabeling and (C,G) EGFP fluorescence. (B-E') The dorsal spinal cord (D,H) and floorplate (E,I) are shown at higher magnification. The expression of full-length PlxnA2 impaired the ventral growth of commissural axons (arrowheads in D). Only EGFP-positive, but no HA-positive, axons were found at the midline (asterisk in E,E'). Note that not all EGFP-positive neurons/axons showed PlxnA2 expression (arrowheads in D',E'), which indicates an inverse relationship between PlxnA2 protein levels in commissural neurons and the ventral projection of their axons. (F-I') PlexinA2ΔCT misexpression did not impair the ventral growth of commissural axons (arrowheads in H,H'). HA-positive axons grew ventrally and crossed the midline (arrowheads in I,I'). Scale bars: 100 μm.

expression of neither PlexinA2ΔmiR nor PlexinA2ΔCTΔmiR rescued the axon guidance phenotypes.

We found an explanation for these unexpected findings when we carefully analyzed commissural axons expressing PlxnA2 constructs. Misexpression of full-length PlxnA2 specifically in dl1 neurons resulted in premature axonal stalling in the dorsal spinal cord in all embryos analyzed ($n=7$), thus preventing the analysis of axonal pathfinding at the ventral midline (Fig. 7B-E'). As PlxnA2 is expressed in pre-crossing axons (Fig. 6E), its levels have to be tightly regulated. Obviously, too much PlxnA2 renders axons sensitive to repellent class-3 semaphorins from the ventral spinal cord, whereas too little PlxnA2 prevents the proper pathfinding of post-crossing axons. Although the overexpression of PlexinA2ΔCT did not affect the ventral axonal trajectory (in all embryos analyzed, $n=7$; Fig. 7F-I'), it nevertheless failed to rescue the post-crossing axon guidance defects (supplementary material Fig. S2D,E).

Taken together, these findings suggest that: (1) the PlxnA2 intracellular domain transduces axonal signals that are required for post-crossing axon pathfinding; and (2) PlxnA2 intracellular signaling is normally inhibited in pre-crossing axons in the ventral spinal cord before floorplate contact to allow growth cone entry into the floorplate. In the dorsal spinal cord, endogenous levels of PlxnA2 are low, as are the levels of repulsive class-3 semaphorins. Therefore, axons extend ventrally. However, when PlxnA2 levels were increased experimentally (Fig. 7B-E), axons were hypersensitive to class-3 semaphorins and failed to extend into the ventral spinal cord.

In summary, our *in vivo* analyses suggest a complex mode of interaction between Sema6B and PlxnA2. As PlxnA2 is required both as a ligand, when expressed on floorplate cells, and as a receptor or co-receptor, when expressed on commissural axons, we suggest the following model (Fig. 8). In the dorsal spinal cord PlxnA2 expressed on pre-crossing commissural axons is not activated by the low levels of repulsive class-3 semaphorins derived from the ventral spinal cord, and axons extend readily towards the floorplate (Fig. 8A). However, in the vicinity of the floorplate, where levels of class-3 semaphorins are high, PlxnA2 on pre-crossing commissural axons is prevented from mediating a

repulsive signal by cis-interaction with Sema6B, which is now expressed on pre-crossing axons of dl1 neurons (Fig. 8B). Upon floorplate contact (Fig. 8C), the cis-complex between axonal PlxnA2 and Sema6B is replaced by a trans-interaction between Sema6B and floorplate PlxnA2. The change from Sema6B-PlxnA2 cis- to trans-interaction mediates a Sema6B-dependent turning signal. Axonal PlxnA2 is available for cis-interaction with neuropilin, resulting in a repulsive signal on post-crossing axons (Nawabi et al., 2010; Parra and Zou, 2010; Zou et al., 2000).

DISCUSSION

Our analyses of Sema6B function in post-crossing commissural axon guidance provide the first report of a receptor function of class-6 semaphorins in vertebrate axon guidance. Our evidence strongly supports the conclusion that Sema6B on commissural axons is the receptor that binds PlxnA2 expressed at the intermediate target: (1) Sema6B is expressed by commissural neurons, PlxnA2 is expressed by floorplate cells, and a direct interaction between Sema6B and PlxnA2 was shown in binding studies and by co-IP; (2) our loss-of-function studies revealed similar defects in post-crossing commissural axon guidance after silencing Sema6B or PlxnA2; (3) the axon guidance effects of Sema6B were dependent on the presence of its intracellular domain; (4) the extracellular domain of PlxnA2 was sufficient to rescue the effects of PlxnA2 knockdown in the floorplate; and (5) a substrate of PlxnA2 ectodomains enhanced the outgrowth of commissural axons in a Sema6B-dependent manner. Although our *in vitro* assay (Fig. 5) did not elucidate the guidance activities of PlxnA2 (because the axons were not faced with a choice of substrate), our results suggest that PlxnA2 is a floorplate-derived ligand that affects axonal behavior in a Sema6B-mediated manner.

A receptor function for class-6 semaphorins is not without precedent. In vertebrates, our previous studies suggested a receptor role of Sema6A in boundary cap cell clustering (Mauti et al., 2007). In addition, Sema6D acts as both ligand and receptor in heart development (Toyofuku et al., 2004a,b). In invertebrates, there is direct evidence that transmembrane semaphorins are axon guidance receptors. Sema1a, which is the closest *Drosophila* homolog of

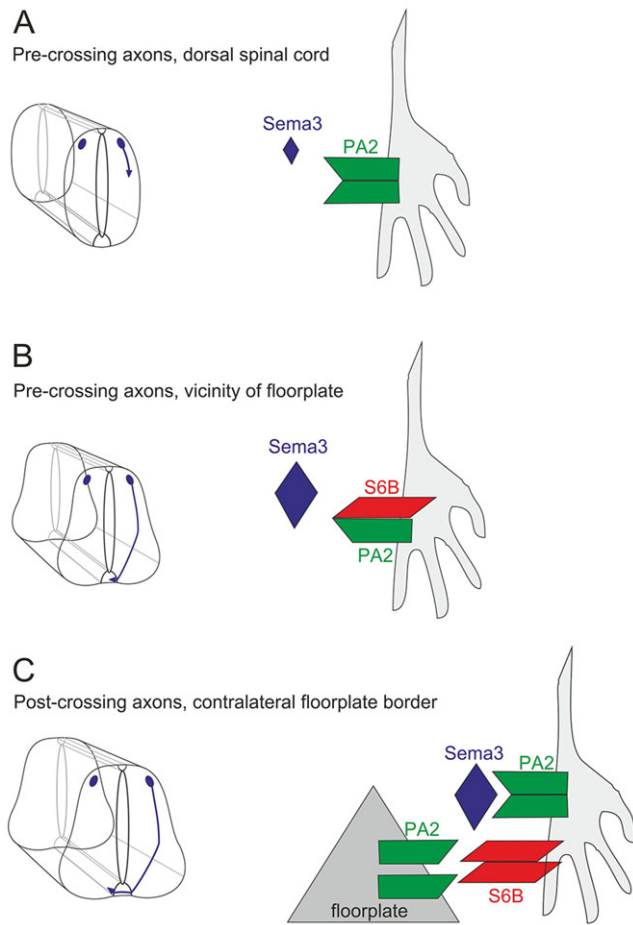


Fig. 8. Model of PlxnA2-Sema6B interactions in commissural axon guidance. (A) In the dorsal spinal cord, pre-crossing axons do not yet express Sema6B. However, axons are not affected by the low levels of repulsive signals (blue diamond) and readily grow towards the ventral midline. Note that we have drawn PlxnA2 (green) arbitrarily as dimer or monomer based on reports on the crystal structures of Sema6A and PlxnA2 (for details see Janssen et al., 2010; Nogi et al., 2010). For simplicity, we omitted neuropilins, which would form complexes with plexins. (B) In the ventral spinal cord, close to the floorplate, where repulsive class-3 semaphorin activity is high (large blue diamond), PlxnA2 (green) is prevented from mediating a repulsive signal due to the cis-interaction with Sema6B (red). (C) At the contralateral floorplate border, post-crossing commissural axons can respond to repulsive class-3 semaphorins, in agreement with published reports (Parra and Zou, 2010; Nawabi et al., 2010), as the cis-interaction of axonal PlxnA2 with Sema6B is replaced by a Sema6B-PlxnA2 trans-interaction. Trans-interactions between floorplate PlxnA2 and growth cone Sema6B result in a turning response and support elongation of post-crossing axons along the contralateral floorplate border.

class-6 semaphorins, was shown to act as a receptor in R-cell axon guidance in the visual system (Cafferty et al., 2006; Yu et al., 2010), in the guidance of projection neurons in the olfactory system (Komiyama et al., 2007) and in motor axon defasciculation (Jeong et al., 2012). Sema1a also acts as both a ligand and receptor in synapse formation (Godenschwege et al., 2002; Godenschwege and Murphey, 2009). However, prior to our current study, the direct evidence that class-6 semaphorins were receptors in vertebrate axon guidance was still missing, despite reports of aberrant axonal decussation in *Sema6a* mutant mice that were suggestive of this function (Leighton et al., 2001; Rünker et al., 2008).

Receptor functions for class-6 semaphorins are in line with their structural characteristics. The C-terminal part of Sema6A contains a zyxin-like domain that represents an Ena/VASP-like protein-

binding site (Klostermann et al., 2000). Ena/VASP proteins regulate actin dynamics and therefore influence neuronal polarization and axon growth (Tahirovic and Bradke, 2009). Ena/VASP-mediated actin dynamics also affect cell migration. Phosphorylation of Ena/VASP by Abl kinase, which was shown to be recruited to the cytoplasmic domain of Sema6D in heart development, is consistent with the observed effects on myocardial cell migration (Toyofuku et al., 2004a).

Because PlxnA2 is not only expressed in the floorplate, but also co-expressed with Sema6B in commissural neurons, the interactions between Sema6B and PlxnA2 might be more complicated than a straightforward receptor-ligand interaction between molecules expressed on the growth cone and floorplate, respectively. In fact, a cis-interaction between Sema6B and PlxnA2 might be part of a regulatory mechanism that controls the sensitivity of commissural axons to repulsive guidance cues in the ventral spinal cord and the floorplate, and may additionally contribute to their switch from attraction to repulsion at the midline.

In line with this idea, a regulatory role of Sema6-plexinA cis-interactions on trans-interactions has been demonstrated in the PNS (Haklai-Topper et al., 2010). Dorsal root ganglion (DRG) axons are not repelled by Sema6A due to the attenuation of Sema6A trans-binding to PlxnA4 by a Sema6A-PlxnA4 cis-interaction. Ablation of Sema6A in DRG axons renders them more susceptible to repulsion by Sema6A. In the same study, Sema6B was identified as a modulator of Sema6A trans-interactions with PlxnA4 (Haklai-Topper et al., 2010). Similarly, an attenuation of the repulsive activity of Sema6A by cis-interacting PlxnA2 has been reported in hippocampal mossy fibers (Suto et al., 2007) and in cerebellar granule cell migration (Renaud et al., 2008).

Our results support the existence of cis-interactions between class-6 semaphorins and plexinAs on commissural axons. A cis-interaction between PlxnA2 and Sema6B might prevent PlxnA2 from interacting with repulsive class-3 semaphorins in the vicinity of the floorplate and, thus, regulate the sensitivity of pre-crossing axons to repulsive cues. Premature sensitivity of pre-crossing axons to class-3 semaphorins would prevent growth cone/floorplate contact and, thus, midline crossing. In agreement with this idea, we found that the overexpression of PlxnA2 in commissural neurons prevented their normal ventral growth (Fig. 7), suggesting that the signaling activity of PlxnA2 is precisely regulated in pre-crossing axons to prevent premature repulsion. Furthermore, our data support the idea that Sema6B-PlxnA2 cis-interactions modulate the binding of PlxnA2 in trans (supplementary material Fig. S5). When axons have reached the midline, floorplate-expressed PlxnA2, which is not involved in any cis-interaction with Sema6B, may bind to growth cone-derived Sema6B in trans, thus inducing a growth/turning signal in the axons. Furthermore, axonal PlxnA2 is freed to interact with class-3 semaphorins derived from the midline. Together, these pathways facilitate the post-crossing trajectory (Fig. 8).

At present, it is not known how the turning signals are mediated intracellularly. However, we propose that the axonal PlxnA2 and Sema6B pathways are separated by the Sema6B-PlxnA2 trans-interaction, resulting in distinct Sema6B- and PlxnA2-mediated parallel signaling in post-crossing axons. This scenario would explain why commissural axons acquire responsiveness to class-3 semaphorins only when crossing the floorplate, but not before. Based on its precise temporal and spatial coincidence with axonal midline crossing, the switch from Sema6B-PlxnA2 cis- to trans-interaction constitutes an excellent regulatory mechanism that contributes to and strengthens the previously described mechanisms: the Shh-induced regulation of PKA activity (Parra and Zou, 2010) and the GDNF-mediated and

NrCAM-dependent inhibition of calpain, which in turn stabilizes PlxnA1 on the growth cone (Nawabi et al., 2010; Charoy et al., 2012).

MATERIALS AND METHODS

Plasmids and miRNAs

Primers for cloning and mutagenesis are listed in supplementary material Table S1; for cloning details see supplementary material methods. miRNA target sequences are listed in supplementary material Table S2. Full-length *Sema6B* (GenBank accession number KJ201030) and a truncated form maintaining the transmembrane region and the five adjacent C-terminal amino acids, but lacking the rest of the intracellular domain, were cloned into pMES (Wilson and Stoeckli, 2011) for *in vivo* studies and into pcDNA3.1 (Invitrogen) for *in vitro* studies. Site-directed mutagenesis (Zheng et al., 2004; Wilson and Stoeckli, 2011) was used to introduce six silent mutations into the miS6B target site of *Sema6b* to make it resistant to knockdown (supplementary material Fig. S1). The same strategy was used to synthesize a knockdown-resistant version of *Plxn2* (supplementary material Fig. S2). Constructs for the expression of miRNAs against *Sema6b* and *Plxn2* were synthesized as described (Wilson and Stoeckli, 2011). GenScript Target Finder was used to predict miRNA target sequences.

In situ probes, dsRNA and immunohistochemistry

Expressed sequence tags (ChESTs) were used to generate dsRNA and *in situ* probes (supplementary material Table S3). *In situ* hybridization and dsRNA synthesis were performed as described (Mauti et al., 2006; Pekarik et al., 2003). Antibodies used for expression analyses on 20 μ m thick cryosections, commissural neurons or HEK293 cells are listed in supplementary material Table S4. Commissural explants were dissected from HH25–26 embryos and cultured on LabTek slides (Nunc, ThermoFisher) coated with poly-L-lysine (10 μ g/ml) and Laminin (10 μ g/ml) as described previously (Niederkofler et al., 2010).

In ovo and in vitro RNAi

After 3 days of incubation at 39°C, fertilized eggs (Hisex) were windowed for injection and electroporation, as described previously (Wilson and Stoeckli, 2011, 2012). Embryos were staged according to Hamburger and Hamilton (1992). All experiments including animals were carried out in accordance with Swiss law on animal experimentation and approved by the cantonal veterinary office of Zurich. Supplementary material Table S5 lists the concentrations and electroporation conditions used. Electrodes were positioned to target one half or the spinal cord (Fig. 3H), or exclusively either dorsal commissural neurons (Fig. 1P) or the ventral midline area (Fig. 3L) (Bourikas et al., 2005; Niederkofler et al., 2010).

The specificity and efficiency of plexin downregulation by the same dsRNA sequences was shown previously (Mauti et al., 2007). The efficiency of gene silencing by miRNAs (supplementary material Figs S1 and S2) was assessed by *in situ* hybridization (Wilson and Stoeckli, 2013) and by *in vitro* screening (Wilson and Stoeckli, 2011). For quantitative analysis of knockdown, the ratio between the signal intensities (grayscale values) of *Sema6B* or *PlxnA2* and the corresponding fluorescent protein from the co-transfected miRNA constructs was calculated using ImageJ (NIH) and subsequently normalized to the miLuc control condition.

Phenotype analysis

Low thoracic and lumbar levels of HH25–26 spinal cords were dissected as open-book preparations to label d11 commissural neurons with Fast-Dil (5 mg/ml in ethanol; D-7756, Life Technologies) as described previously (Perrin and Stoeckli, 2000). An injection site was considered to exhibit a stalling phenotype when more than 50% of the growth cones stalled at the floorplate exit site. Even single axons turning caudally were considered as a ‘caudal turning phenotype’, as caudal turns were only very rarely seen in control embryos. Caudal turning was always seen in combination with axonal stalling at the exit site. Therefore, we did not separate these phenotypes for quantification. No defects in the growth of commissural axons towards the floorplate were observed after *Sema6B* or *PlxnA2* knockdown (supplementary material Fig. S3).

Protein-protein binding experiments

PlxnA1 (aa 31–1040) and PlxnA2 (aa 39–689) ectodomains without the signal peptide were inserted into the pAPtag5 vector (GenHunter) between an Ig κ -chain signal sequence and alkaline phosphatase (AP), followed by a myc/6 \times his tag. For pAPtag5-*PlexinA1* we digested with *SfiI* and *HindIII*, and for pAPtag5-*PlexinA2^{ecto}* with *BglII* and *BspEI*. To obtain pAPtag5-*Sema6B^{ecto}-Fc* (aa 1–590) and pAPtag5-*Sema6A^{ecto}-Fc* (aa 1–604) fusion constructs, we digested pAPtag5 with *BglII* and *BspEI* to insert a human Fc tag with a 3' termination codon. *Sema6A* and *Sema6B* ectodomains were cloned 5' of the Fc tag using *NheI* and *BglII*. Transfection and production of fusion proteins were performed according to published protocols (Flanagan et al., 2000). To assess binding of soluble Plexin^{ecto}-AP fusion proteins, HEK293T cells were transfected with pcDNA3.1-*Sema6A-myc/his*, pCAGGS-*Sema6B-ha* or pCAGGS-*Sema6D-ha* for expression of full-length class-6 semaphorins. Live cells were incubated for 1 hour with Plexin^{ecto}-AP fusion proteins at 4°C before fixation and staining (Flanagan et al., 2000).

For co-IPs, the soluble fusion proteins described above were loaded on Handee spin columns (ThermoFisher) and incubated for 2 hours at 4°C with 10 μ l anti-c-Myc agarose, according to the manufacturer's instructions (ProFound IP-Kit; ThermoFisher, 23620). Immunoprecipitates were analyzed on western blots using the antibodies listed in supplementary material Table S4.

In vitro axon growth assay

Chick embryos at HH17–18 were electroporated with constructs encoding EBFP2 and miLuc or miS6B, as described above. At HH25, dissociated commissural neurons from the electroporated side were collected (pooled from three embryos in each condition) and grown on coverslips pre-coated with poly-L-lysine, which were incubated for 45 min at 37°C with Albumax (50 μ g/ml), Laminin (10 μ g/ml), AP only or PlexinA2^{ecto}-AP (both 50 \times concentrated conditioned medium). Cultures were grown for 48 h before fixation and immunolabeling (Niederkofler et al., 2010) (supplementary material Table S4).

For quantification, at least 20 images per condition were taken from random positions on each coverslip. Each image typically contained both wild-type and miRNA-expressing neurons, which were distinguishable by the expression of EBFP2. At least 34 axons were measured per condition (ImageJ) using a Wacom DTU-1931 tablet and pen tool.

Statistics

For open-books, multiple comparisons by one-way ANOVA followed by Tukey (homoscedasticity) or Tamhane's T2 (heteroscedasticity) post-hoc tests were used to calculate *P*-values, using Statistics-20 Software (SPSS). For the *in vitro* assays we performed two-sample *t*-tests for independent samples using the VassarStats website (<http://vassarstats.net/>). *P*<0.05 was regarded as significant.

Acknowledgements

We thank Tiziana Flego and Dr Beat Kunz for excellent technical support.

Competing interests

The authors declare no competing financial interests.

Author contributions

I.A., N.H.W. and T.B. performed the experiments; I.A., N.H.W., O.M., M.G. and E.T.S. developed the concepts and approach; S.S. provided unpublished constructs; I.A., N.H.W. and E.T.S. performed the data analysis and prepared the manuscript.

Funding

This work was supported by a grant from the Swiss National Science Foundation to E.T.S. and by fellowships of the Roche Research Foundation and the Neuroscience Center Zurich (ZNZ) to I.A. Work in the lab of S.S. was supported by the National Institutes of Health [NS046336].

Supplementary material

Supplementary material available online at <http://dev.biologists.org/lookup/suppl/doi:10.1242/dev.112185/-/DC1>

References

- Augsburger, A., Schuchardt, A., Hoskins, S., Dodd, J. and Butler, S. (1999). BMPs as mediators of roof plate repulsion of commissural neurons. *Neuron* **24**, 127-141.
- Bourikas, D., Pekarik, V., Baeriswyl, T., Grunditz, A., Sadhu, R., Nardó, M. and Stoeckli, E. T. (2005). Sonic hedgehog guides commissural axons along the longitudinal axis of the spinal cord. *Nat. Neurosci.* **8**, 297-304.
- Burstyn-Cohen, T., Tzarfaty, V., Frumkin, A., Feinstein, Y., Stoeckli, E. and Klar, A. (1999). F-Spondin is required for accurate pathfinding of commissural axons at the floor plate. *Neuron* **23**, 233-246.
- Cafferty, P., Yu, L., Long, H. and Rao, Y. (2006). Semaphorin-1a functions as a guidance receptor in the Drosophila visual system. *J. Neurosci.* **26**, 3999-4003.
- Charoy, C., Nawabi, H., Reynaud, F., Derrington, E., Bozon, M., Wright, K., Falk, J., Helmbacher, F., Kindbeiter, K. and Castellani, V. (2012). Gdnf activates midline repulsion by Semaphorin3B via NCAM during commissural axon guidance. *Neuron* **75**, 1051-1066.
- Charron, F., Stein, E., Jeong, J., McMahon, A. P. and Tessier-Lavigne, M. (2003). The morphogen sonic hedgehog is an axonal chemoattractant that collaborates with netrin-1 in midline axon guidance. *Cell* **113**, 11-23.
- Chédotal, A. (2011). Further tales of the midline. *Curr. Opin. Neurobiol.* **21**, 68-75.
- Chen, Z., Gore, B. B., Long, H., Ma, L. and Tessier-Lavigne, M. (2008). Alternative splicing of the Robo3 axon guidance receptor governs the midline switch from attraction to repulsion. *Neuron* **58**, 325-332.
- Domanitskaya, E., Wacker, A., Mauti, O., Baeriswyl, T., Esteve, P., Bovolenta, P. and Stoeckli, E. T. (2010). Sonic hedgehog guides post-crossing commissural axons both directly and indirectly by regulating Wnt activity. *J. Neurosci.* **30**, 11167-11176.
- Eckhardt, F., Behar, O., Calautti, E., Yonezawa, K., Nishimoto, I. and Fishman, M. C. (1997). A novel transmembrane semaphorin can bind c-src. *Mol. Cell. Neurosci.* **9**, 409-419.
- Flanagan, J. G., Cheng, H.-J., Feldheim, D. A., Hattori, M., Lu, Q. and Vanderhaeghen, P. (2000). Alkaline phosphatase fusions of ligands or receptors as in situ probes for staining of cells, tissues, and embryos. *Methods Enzymol.* **327**, 19-35.
- Godenschwege, T. A. and Murphey, R. K. (2009). Genetic interaction of Neuroglian and Semaphorin1a during guidance and synapse formation. *J. Neurogenet.* **23**, 147-155.
- Godenschwege, T. A., Hu, H., Shan-Crofts, X., Goodman, C. S. and Murphey, R. K. (2002). Bi-directional signaling by Semaphorin 1a during central synapse formation in Drosophila. *Nat. Neurosci.* **5**, 1294-1301.
- Haklai-Topper, L., Mlechkovich, G., Savariego, D., Gokhman, I. and Yaron, A. (2010). Cis interaction between Semaphorin6A and Plexin-A4 modulates the repulsive response to Sema6A. *EMBO J.* **29**, 2635-2645.
- Hamburger, V. and Hamilton, H. L. (1992). A series of normal stages in the development of the chick embryo. *Dev. Dyn.* **195**, 231-272.
- Helms, A. W. and Johnson, J. E. (2003). Specification of dorsal spinal cord interneurons. *Curr. Opin. Neurobiol.* **13**, 42-49.
- Islam, S. M., Shinmyo, Y., Okafuji, T., Su, Y., Naser, I. B., Ahmed, G., Zhang, S., Chen, S., Ohta, K., Kiyonari, H. et al. (2009). Draxin, a repulsive guidance protein for spinal cord and forebrain commissures. *Science* **323**, 388-393.
- Janssen, B. J. C., Robinson, R. A., Pérez-Brangulí, F., Bell, C. H., Mitchell, K. J., Siebold, C. and Jones, E. Y. (2010). Structural basis of semaphorin-plexin signalling. *Nature* **467**, 1118-1122.
- Jeong, S., Juhaszova, K. and Kolodkin, A. L. (2012). The Control of semaphorin-1a-mediated reverse signaling by opposing pebble and RhoGAPp190 functions in drosophila. *Neuron* **76**, 721-734.
- Joset, P., Wacker, A., Babey, R., Ingold, E. A., Andermatt, I., Stoeckli, E. T. and Gesemann, M. (2011). Rostral growth of commissural axons requires the cell adhesion molecule MDGA2. *Neural Dev.* **6**, 22.
- Kennedy, T. E., Serafini, T., de la Torre, J. R. and Tessier-Lavigne, M. (1994). Netrins are diffusible chemotropic factors for commissural axons in the embryonic spinal cord. *Cell* **78**, 425-435.
- Kerjan, G., Dolan, J., Haumaitre, C., Schneider-Maunoury, S., Fujisawa, H., Mitchell, K. J. and Chédotal, A. (2005). The transmembrane semaphorin Sema6A controls cerebellar granule cell migration. *Nat. Neurosci.* **8**, 1516-1524.
- Klostermann, A., Lutz, B., Gertler, F. and Behl, C. (2000). The orthologous human and murine semaphorin 6A-1 proteins (SEMA6A-1/Sema6A-1) bind to the enabled/vasodilator-stimulated phosphoprotein-like protein (EVL) via a novel carboxyl-terminal zyxin-like domain. *J. Biol. Chem.* **275**, 39647-39653.
- Kolodkin, A. L. and Tessier-Lavigne, M. (2011). Mechanisms and molecules of neuronal wiring: a primer. *Cold Spring Harb. Perspect. Biol.* **3**, a001727.
- Komiyama, T., Sweeney, L. B., Schuldiner, O., Garcia, K. C. and Luo, L. (2007). Graded expression of semaphorin-1a cell-autonomously directs dendritic targeting of olfactory projection neurons. *Cell* **128**, 399-410.
- Kuwajima, T., Yoshida, Y., Takegahara, N., Petros, T. J., Kumanogoh, A., Jessell, T. M., Sakurai, T. and Mason, C. (2012). Optic chiasm presentation of Semaphorin6D in the context of Plexin-A1 and Nr-CAM promotes retinal axon midline crossing. *Neuron* **74**, 676-690.
- Leighton, P. A., Mitchell, K. J., Goodrich, L. V., Lu, X., Pinson, K., Scherz, P., Skarnes, W. C. and Tessier-Lavigne, M. (2001). Defining brain wiring patterns and mechanisms through gene trapping in mice. *Nature* **410**, 174-179.
- Long, H., Sabatier, C., Ma, L., Plump, A., Yuan, W., Ornitz, D. M., Tamada, A., Murakami, F., Goodman, C. S. and Tessier-Lavigne, M. (2004). Conserved roles for Slit and Robo proteins in midline commissural axon guidance. *Neuron* **42**, 213-223.
- Lyuksyutova, A. I., Lu, C.-C., Milanesio, N., King, L. A., Guo, N., Wang, Y., Nathans, J., Tessier-Lavigne, M. and Zou, Y. (2003). Anterior-posterior guidance of commissural axons by Wnt-frizzled signaling. *Science* **302**, 1984-1988.
- Mambetisaeva, E. T., Andrews, W., Camurri, L., Annan, A. and Sundaresan, V. (2005). Robo family of proteins exhibit differential expression in mouse spinal cord and Robo-Slit interaction is required for midline crossing in vertebrate spinal cord. *Dev. Dyn.* **233**, 41-51.
- Mauti, O., Sadhu, R., Gemayel, J., Gesemann, M. and Stoeckli, E. T. (2006). Expression patterns of plexins and neuropilins are consistent with cooperative and separate functions during neural development. *BMC Dev. Biol.* **6**, 32.
- Mauti, O., Domanitskaya, E., Andermatt, I., Sadhu, R. and Stoeckli, E. T. (2007). Semaphorin6A acts as a gate keeper between the central and the peripheral nervous system. *Neural Dev.* **2**, 28.
- Nawabi, H. and Castellani, V. (2011). Axonal commissures in the central nervous system: how to cross the midline? *Cell. Mol. Life Sci.* **68**, 2539-2553.
- Nawabi, H., Briancon-Marjollet, A., Clark, C., Sanyas, I., Takamatsu, H., Okuno, T., Kumanogoh, A., Bozon, M., Takeshima, K., Yoshida, Y. et al. (2010). A midline switch of receptor processing regulates commissural axon guidance in vertebrates. *Genes Dev.* **24**, 396-410.
- Niederkofler, V., Baeriswyl, T., Ott, R. and Stoeckli, E. T. (2010). Nectin-like molecules/SynCAMs are required for post-crossing commissural axon guidance. *Development* **137**, 427-435.
- Nogi, T., Yasui, N., Mihara, E., Matsunaga, Y., Noda, M., Yamashita, N., Toyofuku, T., Uchiyama, S., Goshima, Y., Kumanogoh, A. et al. (2010). Structural basis for semaphorin signalling through the plexin receptor. *Nature* **467**, 1123-1127.
- Parra, L. M. and Zou, Y. (2010). Sonic hedgehog induces response of commissural axons to Semaphorin repulsion during midline crossing. *Nat. Neurosci.* **13**, 29-35.
- Pasterkamp, R. J. (2012). Getting neural circuits into shape with semaphorins. *Nat. Rev. Neurosci.* **13**, 605-618.
- Pasterkamp, R. J. and Kolodkin, A. L. (2003). Semaphorin junction: making tracks toward neural connectivity. *Curr. Opin. Neurobiol.* **13**, 79-89.
- Pekarik, V., Bourikas, D., Miglino, N., Joset, P., Preiswerk, S. and Stoeckli, E. T. (2003). Screening for gene function in chicken embryo using RNAi and electroporation. *Nat. Biotechnol.* **21**, 93-96.
- Perrin, F. E. and Stoeckli, E. T. (2000). Use of lipophilic dyes in studies of axonal pathfinding in vivo. *Microsc. Res. Tech.* **48**, 25-31.
- Philipp, M., Niederkofler, V., Debrunner, M., Alther, T., Kunz, B. and Stoeckli, E. T. (2012). RabGDI controls axonal midline crossing by regulating Robo1 surface expression. *Neural Dev.* **7**, 36.
- Renaud, J., Kerjan, G., Sumita, I., Zagar, Y., Georget, V., Kim, D., Fouquet, C., Suda, K., Sanbo, M., Suto, F. et al. (2008). Plexin-A2 and its ligand, Sema6A, control nucleus-centrosome coupling in migrating granule cells. *Nat. Neurosci.* **11**, 440-449.
- Rünker, A. E., Little, G. E., Suto, F., Fujisawa, H. and Mitchell, K. J. (2008). Semaphorin-6A controls guidance of corticospinal tract axons at multiple choice points. *Neural Dev.* **3**, 34.
- Sabatier, C., Plump, A. S., Ma, L., Brose, K., Tamada, A., Murakami, F., Lee, E. Y.-H. P. and Tessier-Lavigne, M. (2004). The divergent Robo family protein rig-1/Robo3 is a negative regulator of slit responsiveness required for midline crossing by commissural axons. *Cell* **117**, 157-169.
- Stoeckli, E. T. and Landmesser, L. T. (1995). Axonin-1, Nr-CAM, and Ng-CAM play different roles in the in vivo guidance of chick commissural neurons. *Neuron* **14**, 1165-1179.
- Stoeckli, E. T., Sonderegger, P., Pollerberg, G. E. and Landmesser, L. T. (1997). Interference with axonin-1 and NrCAM interactions unmasks a floor-plate activity inhibitory for commissural axons. *Neuron* **18**, 209-221.
- Suto, F., Ito, K., Uemura, M., Shimizu, M., Shinkawa, Y., Sanbo, M., Shinoda, T., Tsuboi, M., Takashima, S., Yagi, T. et al. (2005). Plexin-a4 mediates axon-repulsive activities of both secreted and transmembrane semaphorins and plays roles in nerve fiber guidance. *J. Neurosci.* **25**, 3628-3637.
- Suto, F., Tsuboi, M., Kamiya, H., Mizuno, H., Kiyama, Y., Komai, S., Shimizu, M., Sanbo, M., Yagi, T., Hiromi, Y. et al. (2007). Interactions between plexin-A2, plexin-A4, and semaphorin 6A control lamina-restricted projection of hippocampal mossy fibers. *Neuron* **53**, 535-547.
- Tahirovic, A. and Bradke, F. (2009). Neuronal polarity. *Cold Spring Harb. Perspect. Biol.* **1**, a001644.
- Tawarayama, H., Yoshida, Y., Suto, F., Mitchell, K. J. and Fujisawa, H. (2010). Roles of semaphorin-6B and plexin-A2 in lamina-restricted projection of hippocampal mossy fibers. *J. Neurosci.* **30**, 7049-7060.

- Toyofuku, T., Zhang, H., Kumanogoh, A., Takegahara, N., Yabuki, M., Harada, K., Hori, M. and Kikutani, H.** (2004a). Guidance of myocardial patterning in cardiac development by Sema6D reverse signalling. *Nat. Cell Biol.* **6**, 1204-1211.
- Toyofuku, T., Zhang, H., Kumanogoh, A., Takegahara, N., Suto, F., Kamei, J., Aoki, K., Yabuki, M., Hori, M., Fujisawa, H. et al.** (2004b). Dual roles of Sema6D in cardiac morphogenesis through region-specific association of its receptor, Plexin-A1, with off-track and vascular endothelial growth factor receptor type 2. *Genes Dev.* **18**, 435-447.
- Toyofuku, T., Yoshida, J., Sugimoto, T., Yamamoto, M., Makino, N., Takamatsu, H., Takegahara, N., Suto, F., Hori, M., Fujisawa, H. et al.** (2008). Repulsive and attractive semaphorins cooperate to direct the navigation of cardiac neural crest cells. *Dev. Biol.* **321**, 251-262.
- Wilson, N. H. and Stoeckli, E. T.** (2011). Cell type specific, traceable gene silencing for functional gene analysis during vertebrate neural development. *Nucleic Acids Res.* **39**, e133.
- Wilson, N. H. and Stoeckli, E. T.** (2012). In ovo electroporation of miRNA-based plasmids in the developing neural tube and assessment of phenotypes by Dil injection in open-book preparations. *J. Vis. Exp.* e4384.
- Wilson, N. H. and Stoeckli, E. T.** (2013). Sonic hedgehog regulates its own receptor on postcrossing commissural axons in a glypican1-dependent manner. *Neuron* **79**, 478-491.
- Xu, X. M., Fisher, D. A., Zhou, L., White, F. A., Ng, S., Snider, W. D. and Luo, Y.** (2000). The transmembrane protein semaphorin 6A repels embryonic sympathetic axons. *J. Neurosci.* **20**, 2638-2648.
- Yu, L., Zhou, Y., Cheng, S. and Rao, Y.** (2010). Plexin a-semaphorin-1a reverse signaling regulates photoreceptor axon guidance in Drosophila. *J. Neurosci.* **30**, 12151-12156.
- Zheng, L., Baumann, U. and Reymond, J.-L.** (2004). An efficient one-step site-directed and site-saturation mutagenesis protocol. *Nucleic Acids Res.* **32**, e115.
- Zhuang, B., Su, Y. S. and Sockanathan, S.** (2009). FARP1 promotes the dendritic growth of spinal motor neuron subtypes through transmembrane Semaphorin6A and PlexinA4 signaling. *Neuron* **61**, 359-372.
- Zou, Y., Stoeckli, E., Chen, H. and Tessier-Lavigne, M.** (2000). Squeezing axons out of the gray matter: a role for slit and semaphorin proteins from midline and ventral spinal cord. *Cell* **102**, 363-375.

Supplementary Material

Supplementary Methods

Table S1. Primers used for cloning and site-directed mutagenesis

Clone	Forward primer (5'-3')	Reverse primer (5'-3')
Sema6B, full cDNA	ATGTGGCCCCCCTCGTC	CTATTTGCCCGAGGGAGTC
Sema6D, full cDNA	ATGAGGCTTCCTCTGCTGTG	CTAGTAACTGTATTTGTTCAAGTGGTC TGA
Sema6B ΔmiR	GGAAGCTCACATGGCGATCCAATCA GCACGACATCAGCATC	CACGTGCTGATTGGATCGCCATGTGA GCTTCCGGTGATAGCG
PlexinA2 ΔmiR	GGAAGCTGTTTCATAGGGACCGCTGTG GATGGGAAGC	CCACAGCGGTCCCTATGAACAGCT TCCCATCCTCG

To clone Sema6B into the pCAGGs vector, we added XbaI and BglII restriction sites to the forward and reverse primer, respectively. In addition, the forward primer contained the Kozak sequence (5'-GCCACCATGG) and the reverse primer was modified with an in-frame HA-tag sequence. The full-length Sema6BΔmiR and truncated Sema6BΔmiR version (lacking the intracellular sequence but maintaining the transmembrane domain and the first five intracellular amino acids) were inserted into the pMES-IRES-EGFP vector using XbaI and BglII restriction sites for the insert, and XbaI and BamHI for the vector. With the same restrictions sites we cloned the myc/his-tagged Sema6B constructs into pcDNA3.1 for *in vitro* assays. Similarly, full-length chicken PlexinA2ΔmiR and truncated PlexinA2ΔCTΔmiR (aa 1-1259) were cloned into pMath1-IRES-EGFP for specific expression in dl1 neurons (Wilson and Stoeckli, 2011).

Table S2. Target sequences of artificial miRNAs used in this study

Gene	Target sequence (5'-3')	Comment/Reference
Sema6B	AAGCTGACTTGGAGGTCGAACC	
PlexinA2	AAGCTCTTCATTGGCACGGCA	
Firefly Luciferase	CGTGGATTACGTCGCCAGTCAA	Wilson and Stoeckli, 2011

Table S3. ChESTs and cDNAs used to generate *in situ* hybridization probes and/or dsRNA

Gene	ChEST	Comment/Reference
Semaphorin6B	cDNA fragment	Mauti et al., 2006 and 2007
Semaphorin6D	225N10	ChEST
PlexinA1	53D13, 666O16	ChESTs
PlexinA2	128L21, 297D11	ChESTs
PlexinA4	1014M19, 202O14	ChESTs
Sonic hedgehog (Shh)	cDNA fragment	Bourikas et al., 2005
Slit2	cDNA fragment	Philipp et al., 2012

Chicken ESTs were purchased from Source BioScience LifeSciences, Nottingham, UK.

Table S4. Antibodies used in this study

Primary antibodies		
Protein detected	Antibody	Company/Source
myc-tagged Sema6B	mouse anti-Myc (9E10; hybridoma supernatant)	Developmental Studies Hybridoma Bank, Iowa City, IA, USA
HA-tagged PlexinA2	rabbit anti-HA (1:2,000)	Rockland Immunochemicals #600-401-384 Gilbertsville, PA, USA
Axonin1/Contactin2	rabbit anti-Axonin1 (1:1000)	Stoeckli and Landmesser, 1995
PlexinA1	rabbit anti-PlexinA1 (1:200)	Atlas Antibodies, #HPA007499, Stockholm, Sweden
PlexinA2	goat anti-PlexinA2 (1:200)	R&D Systems, #AF5486 Abingdon, UK
PlexinA4	rabbit anti-PlexinA4 (1:200)	Abcam, #ab39350 Cambridge, UK
Sema6B	goat anti-Sema6B (1:20)	R&D Systems, #AF2094
EBFP2	Fluorescein-conjugated goat anti-GFP (1:500)	Rockland Immunochemicals, #600-102-215
Hnf3β	mouse anti-Hnf3 β (4C7; hybridoma supernatant)	DSHB
Nkx2.2	mouse anti-Nkx2.2 (74.5A5; conc. supernatant)	DSHB
Neurofilament	mouse anti-Neurofilament (4H6; supernatant)	DSHB
Fc-tagged Sema6 (Western blot)	Alexa-488 goat anti-human IgG (1:10,000)	Invitrogen, #A11013 Paisley, UK
Secondary antibodies		
Mouse IgG	donkey anti-mouse IgG-Cy3 (1:250)	Jackson ImmunoResearch, #715-165-150 West Grove, PA, USA
Mouse IgG	goat anti-mouse IgG-Alexa488 (1:250)	Invitrogen, #A11001
Rabbit IgG	donkey anti-rabbit IgG-Cy3 (1:250)	Jackson ImmunoResearch, #711-165-152
Goat IgG	donkey anti-goat IgG-Cy3 (1:250)	Jackson ImmunoResearch #705-165-147

Mouse IgG (Western blot)	sheep anti-mouse peroxidase (1:10,000)	Sigma-Aldrich, #A6782 St.Louis, MO, USA
Goat IgG (Western blot)	rabbit anti-goat peroxidase (1:10,000)	MP Biomedicals, #55358 Santa Ana, CA, USA

Table S5. Concentrations and *in vivo* electroporation parameters used in this study

Experiment/Figure	Concentration	Electroporation Parameters
Fig.1; Fig. 3; Fig. 6 (Long dsRNA)	300 ng/ μ l dsRNA 20 ng/ μ l EGFP plasmid	Unilateral, dorsal or ventral targeting (manual positioning) 5 x 50 ms pulses; 25 V
Fig. 2; Fig. S1 (miS6B, rescue constructs)	300 ng/ μ l miRNA construct 500 ng/ μ l rescue construct	Unilateral or dorsal targeting (manual positioning) 5 x 50 ms pulses; 25 V
Fig. 4 (miPA2, rescue constructs)	1 μ g/ μ l miRNA construct 1 μ g/ μ l rescue construct	Floorplate-specific targeting (<i>Hoxa-1</i> enhancer-driven) Bilateral; for each side: 5 x 50 ms pulses; 18V
Fig. 5, Fig. S2K (miS6B, miLuc)	300 ng/ μ l miRNA construct	Unilateral targeting 5 x 50 ms pulses; 25 V
Fig. 7, Fig. S2B-E (miPA2, rescue constructs)	600 ng/ μ l miRNA construct 350 ng/ μ l rescue construct	dI1 neuron-specific targeting (<i>Math1</i> enhancer-driven) 5 x 50 ms pulses; 25 V

In ovo RNAi with long dsRNA was used where possible, as it is the most efficient method for specific gene silencing. Where required, for example for exclusive targeting of dI1 commissural neurons or for rescue experiments, we used miR constructs.

Supplementary Figures

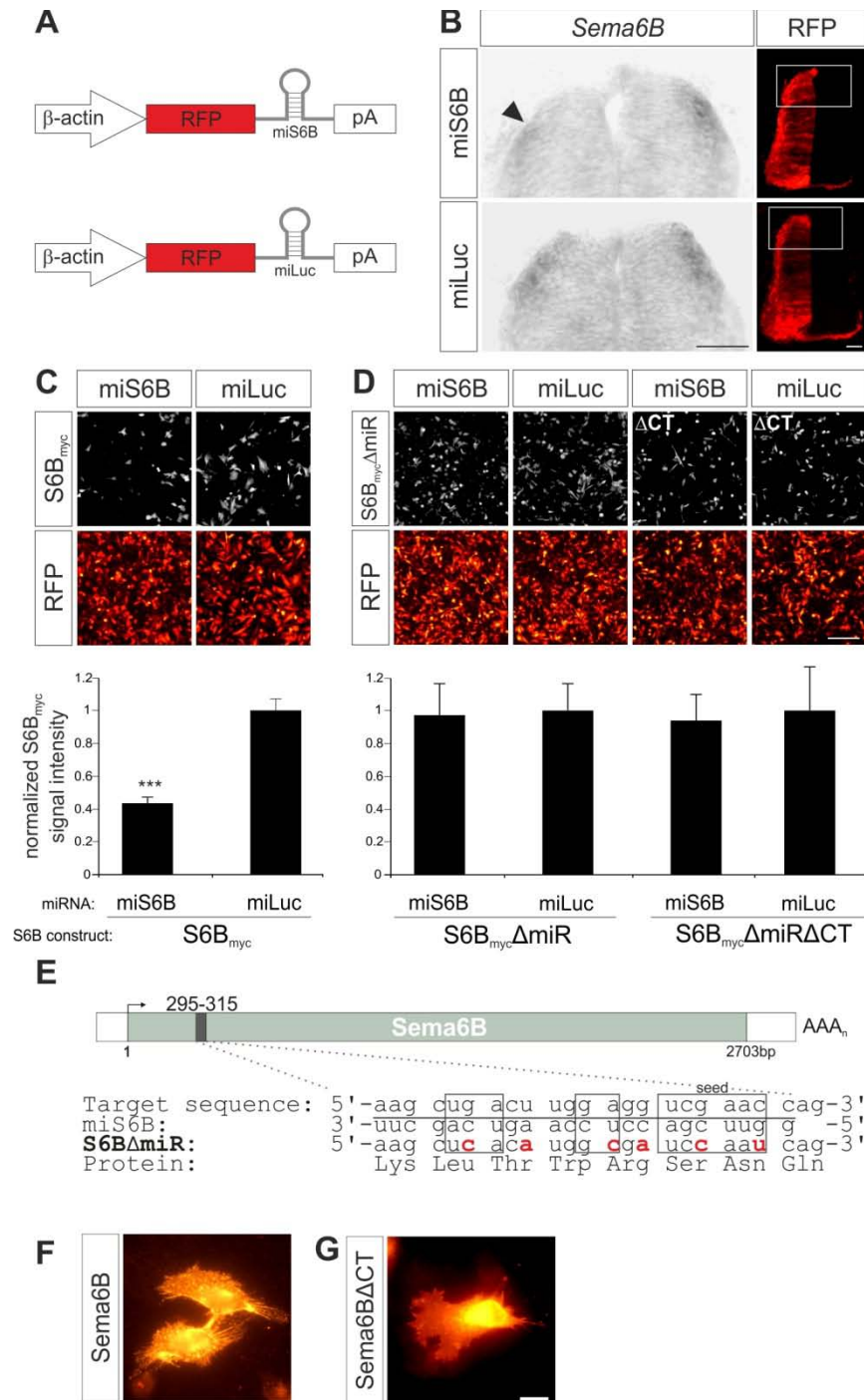


Figure S1

Figure S1. miS6B efficiently downregulates wild-type Sema6B *in vivo* and *in vitro*, but Sema6B containing a mutated miRNA target sequence is resistant to knockdown.

(A) Schematic representations of microRNA constructs against Sema6B (miS6B) and Luciferase (miLuc). (B) *Sema6B* ISH on transverse spinal cord sections taken from embryos expressing miS6B or miLuc. Electroporation of miS6B reduced expression of *Sema6B* on the electroporated side (arrowhead) by $80.5 \pm 6.1\%$ (s.e.m.) compared to the control side ($n=4$ sections from two embryos; $p < 0.0005$, t-test). In contrast, electroporation of miLuc did not significantly affect *Sema6B* expression (staining reduced by $12.4 \pm 17.0\%$ (s.e.m.) on the electroporated side compared to the control side; $n=5$ sections from four embryos; $p=0.253$, t-test). Transfection was visualized by RFP. Scale bar, 50 μm . (C) miS6B efficiently reduced expression of Sema6B in HeLa cells. Myc-tagged Sema6B ($S6B_{\text{myc}}$) was reduced by almost 60% when co-transfected with miS6B compared to miLuc. $n=28$ measurements each; $***p < 0.001$, t-test. (D) miS6B did not reduce the expression of Sema6B Δ miR or Sema6B Δ CT Δ miR, two knockdown-resistant forms of Sema6B. The co-transfection of Sema6B Δ miR or Sema6B Δ CT Δ miR with either control miLuc or miS6B did not exhibit any significant change in Sema6B/RFP intensity ratios. Ratios were normalized to miLuc control. Scale bars, 100 μm . (E) Design of miRNA-resistant Sema6B for rescue experiments. The region of the Sema6B mRNA that is targeted by miS6B is underlined. Regions important for miRNA target selection and cleavage are indicated by boxes. A miRNA-resistant version of Sema6B (Sema6B Δ miR) was generated by silent mutagenesis of 6 bases in the target region (red). The encoded protein sequence was unaltered. (F) Surface staining of transfected cells revealed that both full-length Sema6B and (G) Sema6B Δ CT constructs were efficiently expressed in HEK293 cells and correctly targeted to the membrane (see also Fig.4M). Scale bar, 5 μm .

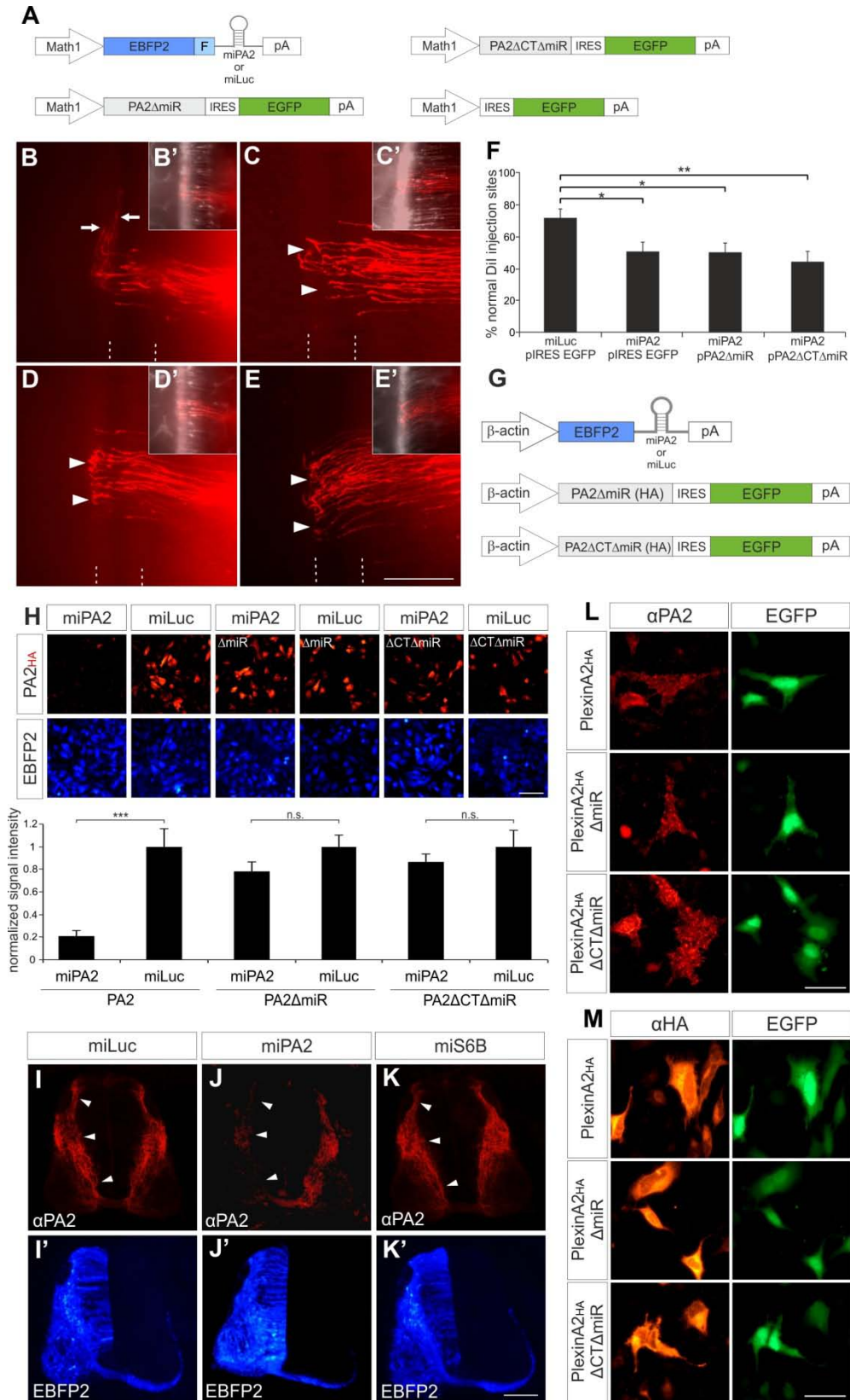


Figure S2

Figure S2. PlexinA2 influences the extension of commissural axons into the ventral spinal cord and their post-crossing turning decision. The PlexinA2 miRNAs and rescue constructs perform as expected.

(A) Schematics of constructs used for dl1 neuron-specific perturbations of PlexinA2. (B) In control embryos co-electroporated with dl1-specific constructs encoding EBFP2-miLuc and the empty *pMath1-IRES-EGFP* plasmid, commissural axons crossed the floorplate and turned rostrally (arrows). (C) Knocking down PlexinA2 with miPA2 resulted in stalling of post-crossing axons at the contralateral floorplate border (arrowheads). The phenotype caused by miPA2 was not rescued by the co-electroporation of PlexinA2ΔmiR (D) or by PlexinA2 lacking the cytoplasmic tail (PlexinA2ΔCTΔmiR) (E; arrowheads). The floorplate is indicated by dashed lines. (B'-E') Merge of Dil-labeled axons (red) and farnesylated EBFP2 (white) used to visualize the expression of different miRNA constructs (EGFP not shown). (F) Quantification of Dil sites with normal axonal pathfinding: control (n=8 embryos, N= 71 injection sites); knock down (n=16, N=137); full-length rescue (n=25, N=228); ΔCT rescue (n=11, N=108). * $p < 0.05$, ** $p < 0.01$. (G) Schematic representations of the constructs used in the verification of miPA2 and PA2ΔmiR constructs. (H) HA-tagged PlexinA2 was reduced by almost 80% when co-transfected with miPA2, compared to miLuc (** $p < 0.001$; n=11 and 13 measurements, respectively). However, miPA2 did not reduce the expression of PlexinA2ΔmiR and PlexinA2ΔCTΔmiR, since both constructs contained several silent mutations in the miPA2 target sequence (see Methods). Co-transfection of PlexinA2ΔmiR or PlexinA2ΔCTΔmiR with either control miLuc or miPA2 did not exhibit any significant change in PlexinA2/EBFP2 intensity ratios (12-16 measurements in each condition). Ratios were normalized to miLuc control. Scale bars, 100 μm. (I-K) The downregulation of PlexinA2 upon electroporation of miLuc, miPA2 or miS6B was assessed by PlexinA2 immunoreactivity. In control embryos electroporated with miLuc (I), PlexinA2 expression in pre-crossing commissural axons was no different from the control side. In contrast, PlexinA2 was clearly reduced after electroporation of miPA2 (J, arrowheads). Expression of miS6B (K) did not affect surface levels of PlexinA2 in pre-crossing axons. (I'-K') Successful transfection is visualized by EBFP2 expression. (L-M) Surface and total expression of wildtype and knockdown-resistant PlexinA2 in HEK293 cells. (L) Surface expression was demonstrated by staining HEK293 cells with a PlexinA2 antibody before fixation and permeabilization. Successful transfection was demonstrated by EGFP expression from the same plasmid. (M) For staining total levels of the expressed PlexinA2, cells were fixed and stained with an antibody against the C-terminal HA-tag. Scale bars, 20 μm.

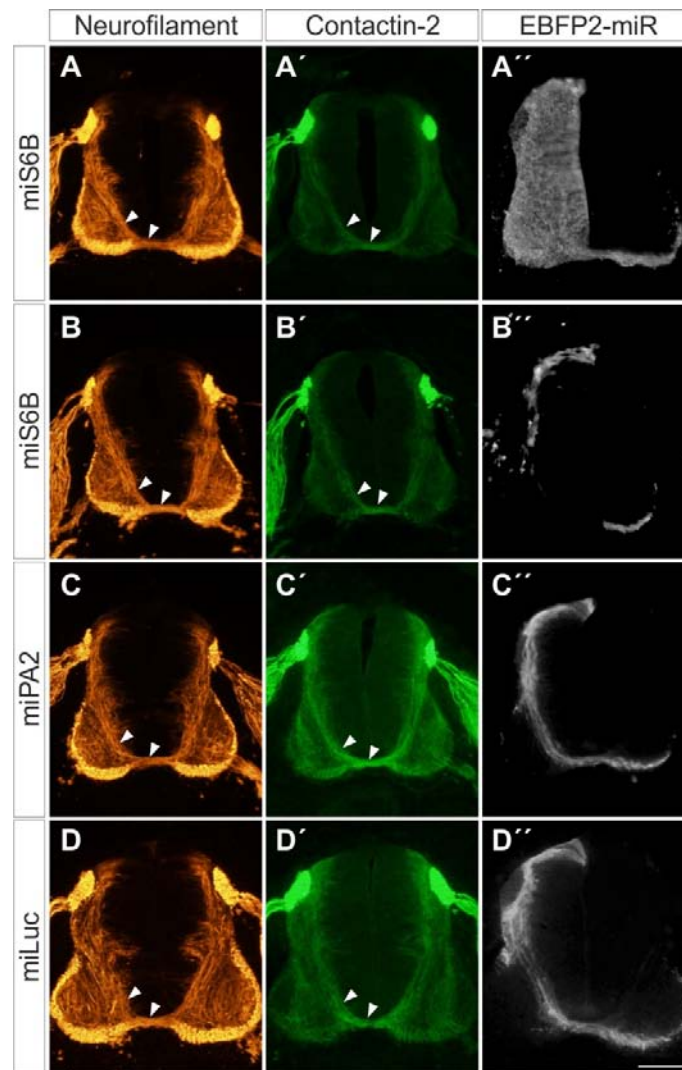


Figure S3

Figure S3. Commissural axon outgrowth is not grossly impaired following the loss of PlexinA2 or Sema6B.

To verify that pre-crossing commissural axon projections were grossly normal following the loss of PlexinA2 or Sema6B, transverse sections of the chicken spinal cord were immunolabeled for neurofilament (A-D) and Axonin1/Contactin2 (A'-D'). Neither unilateral (A-A'') nor dorsal (B-B'') downregulation of Sema6B impaired the ventral growth of commissural axons compared to controls (D-D''). Similarly, no defects in the ventral projection of commissural axons were observed when PlexinA2 was specifically downregulated in d11 neurons with Math1-miPA2 (C-C''). Scale bar, 100 μ m.

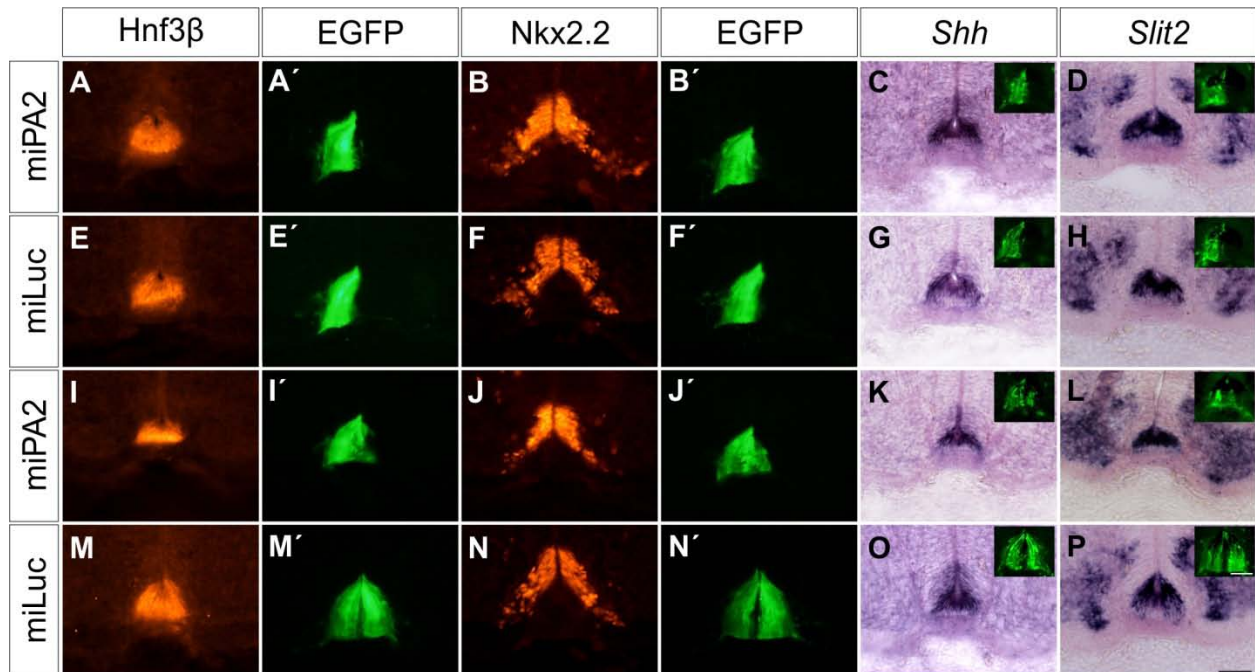


Figure S4

Figure S4. Downregulation of PlexinA2 in the floorplate does not interfere with floorplate morphology or the expression of other axon guidance cues.

To control for a direct effect on commissural axon guidance of PlexinA2 silencing in the floorplate, we analyzed marker expression in the ventral spinal cord after unilateral (A-H) or bilateral (I-P) electroporation of floorplate-specific constructs encoding miPA2 or miLuc. No differences were seen in any condition when we analyzed Hnf3 β (A,E,I,M) or Nkx2.2 (B,F,J,N). Similarly, no changes in the expression of *Shh* (C,G,K,O) or *Slit2* (D,H,L,P) were observed. Successful electroporation was verified by GFP expression (A'-N', and insets). Scale bar, 50 μ m.

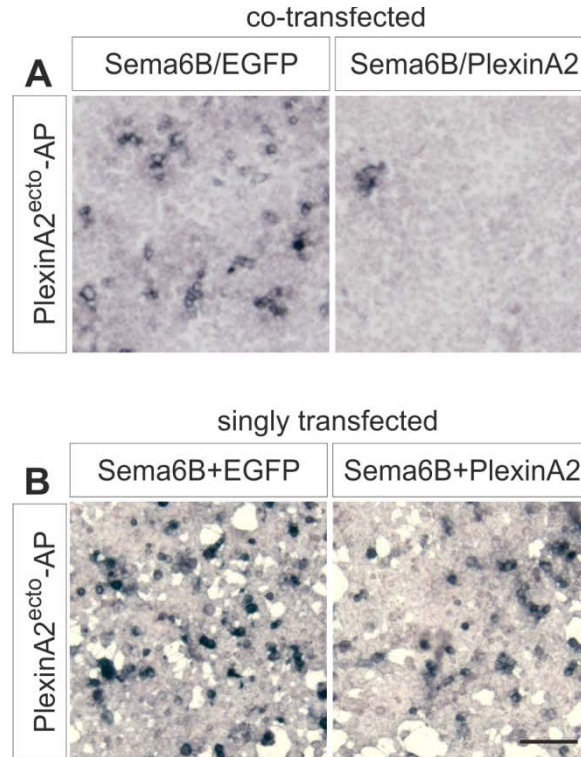


Figure S5

Figure S5. Sema6B/PlexinA2 cis-interaction modulates Sema6B/PlexinA2 trans-interaction.

We assessed the binding of PlexinA2^{ecto}-AP on HEK293 cells transfected with vectors expressing Sema6B and EGFP, or Sema6B and PlexinA2. In panel (A), the cells were co-transfected with the indicated constructs, promoting the formation of cis-complexes. The binding of PlexinA2^{ecto}-AP to Sema6B/PlexinA2 co-transfected cells was markedly reduced compared to binding on Sema6B/EGFP-expressing cells. In panel (B), the cells were separately transfected with Sema6B, EGFP or PlexinA2 and then mixed and replated in the combinations indicated. After single transfections (minimal cis-interactions), the binding of PlexinA2^{ecto}-AP to Sema6B + EGFP cells was comparable to Sema6B + PlexinA2 cells. Scale bar, 100 μ m.